CR-135182

National Aeronautics and Space Administration

ENVIRONMENTAL EFFECTS ON ALUMINUM FRACTURE

by Fred R. Schwartzberg and John A. Shepic

MARTIN MARIETTA CORPORATION

prepared for

NATIONAL AERONAUTICS AND SPACE ADMINISTRATION

NASA Lewis Research Center
Contract NAS3-18923

1. Report No. CR-135182	2. Government Accession No.	3 Recipient's Catalog No
4. Title and Subtitle ENVIRONMENTAL EFFECTS ON ALUMINUM FRACTURE		5 Report Date August 1976
		6. Performing Organization Code
7. Author(s) F. R. Schwartzberg and John A. Shepic		8 Performing Organization Report No MCR-76-385
9. Performing Organization Name and Address Martin Marietta Corporation Denver, Colorado 80201		10 Work Unit No
		11 Contract or Grant No. NAS3-18923
12 Sponsoring Agency Name and Address National Aeronautics and Space Administration Washington, D.C. 20546		13 Type of Report and Period Covered Contractor Report
		14 Sponsoring Agency Code

15 Supplementary Notes

Project Managers, John A. Misencik and G. T. Smith, NASA Lewis Research Center, Cleveland, Ohio

16 Abstract This work was to determine the sustained load stress corrosion cracking (SCC) threshold for aluminum alloy 2124 using smooth (σ_{TH}) and precracked (K_{ISCC}) specimens and the cyclic load growth behavior in 3.5% NaCℓ salt solution. The relationship between K_{ISCC} and σ_{TH} was also to be studied. The work showed that 2124-T851 aluminum alloy in plate gage has a moderately high resistance to stress corrosion attack.

Experimental results showed that no SCC was found for the longitudinal and long transverse directions in any of the tests; SCC was found by smooth tests in the short transverse direction, and the data were confirmed by two test methods-- $\sigma_{TH} = 275\ MN/m^2$ (40 ksi); no SCC was found from compact specimen tests in any direction; surface-flaw and center-notch specimens evaluated in the short transverse direction exhibited SCC. The data indicate that stress corrosion behavior is defect, size, and stress dependent, but not entirely in accordance with a stress-intensity-controlled mechanism.

17. Key Words	18. Distribution Statement Unclassified - unlimited

19. Security Classif. (of this report)	20. Security Classif. (of this page)	21. No. of Pages	22. Price
Unclassified	Unclassified		

PAGES MISSING FROM AVAILABLE VERSION

FOREWORD

This report describes the results of a program to study the stress corrosion behavior of 2124-T851 aluminum alloy. The program was conducted by Martin Marietta Corporation, Denver Division, under NASA Contract NAS3-18923.

This work was performed under the management of NASA Project Managers John A. Mesincik and Gordon T. Smith.

The Martin Marietta Program Manager for the activity was Fred R. Schwartzberg. Mr. John A. Shepic served as Principal Investigator.

PAGES MISSING FROM AVAILABLE VERSION

CONTENTS

FIGURES

TABLES

SUMMARY

The work described was undertaken to determine the sustained load stress corrosion cracking (SCC) threshold for aluminum alloy 2124 using smooth (σ_{TH}) and precracked (K_{ISCC}) specimens and the cyclic load growth behavior in 3.5% NaCℓ salt solution. The relationship between K_{ISCC} and σ_{TH} was also studied.

The results of the work showed that 2124-T851 aluminum alloy in plate gage has a moderately high resistance to stress corrosion attack.

Experimental results showed that:

1) No SCC was found for the longitudinal and long transverse directions in any of the tests;
2) SCC was found by smooth tests in the short transverse direction, and the data were confirmed by two test methods-- σ_{TH} = 275 MN/m^2 (40 ksi);
3) No SCC was found from compact specimen tests in any direction;
4) Surface-flaw and center-notch specimens evaluated in the short transverse direction exhibited SCC;
5) Cyclic crack growth tests showed a directionality effect and a minor effect of environment on growth rates.

The data indicate that stress corrosion behavior depends on defect size and stress, but not entirely in accordance with a stress-intensity controlled mechanism.

PAGES MISSING FROM AVAILABLE VERSION

INTRODUCTION

During recent years, the fracture mechanics approach to studying stress corrosion cracking (SCC) using precracked specimens has become popular. The traditional approach, using smooth stressed specimens, although somewhat less popular now, still receives attention, but is a slow procedure that requires careful evaluation. The normal smooth-specimen testing process involves long-term loading of a number of specimens at varying load levels until failure or visual evidence of cracking occurs. Frequently, metallographic examination is required to verify threshold selections. Figure 1 shows typical SCC data for alternate immersion testing of 7075-T6 aluminum alloy in 3.5% $NaC\ell$ using smooth specimens. Data points have been deleted for clarity. A typical series of tests frequently involves more than 100 tests per grain orientation. The data clearly show the low short transverse resistance $\left(\sigma_{TH} = 48 \text{ MN/m}^2 \text{ (7 ksi)}\right)$. Similarly, Figure 2 presents data for precracked specimens used to generate a K_{ISCC} level for 7075-T6 in the short transverse direction only. The stress intensity threshold is only 7 $\text{MN/m}^{3/2}$ (6 ksi $\sqrt{\text{in.}}$). Note that the concept of the existence of a stress intensity threshold for alluminum alloys is subject to some doubt. Crack growth rates, while becoming very low, are still finite. Hence, the threshold concept may best be considered as an engineering design expediency.

Because both precracked and smooth specimen tests are in use, an understanding of the relationships among the results is highly desirable to avoid overdesign and/or inadequate stress corrosion resistance of critical structural components.

For smooth testing, nominal stress governs the threshold level for initiation of stress corrosion cracking. The fracture mechanics approach, using precracked specimens, is predicated on the intensity of the crack tip stress field or the nominal stress and crack size governing the threshold for stress corrosion crack propagation. A relationship that unifies the nominal and local stress concepts is required in order to use SCC data in design applications.

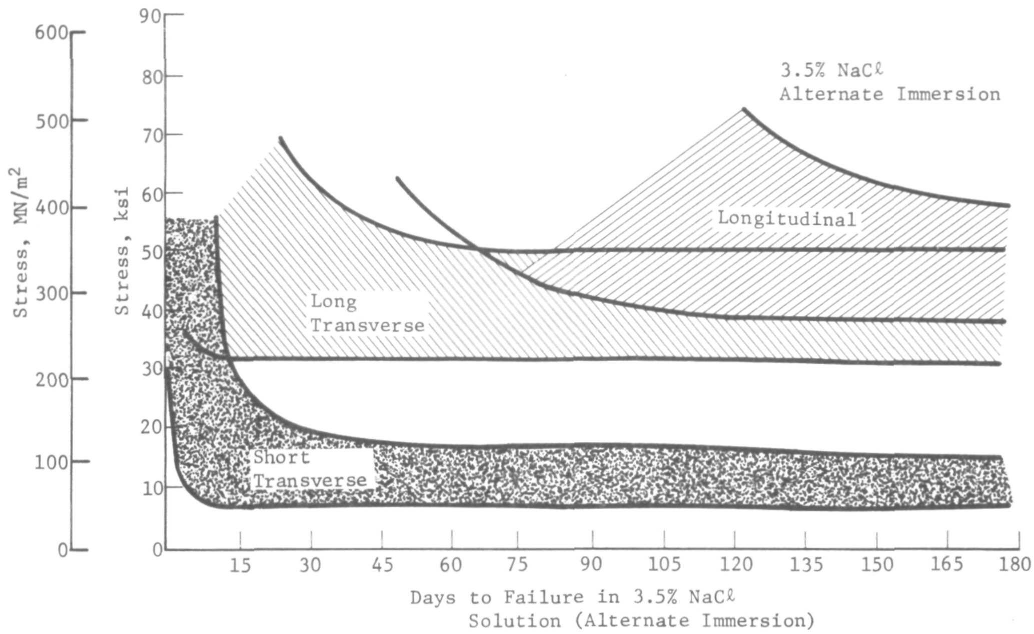

Figure 1.- Stress corrosion data for 7075-T6 aluminum (smooth specimens) [Sprowels and Brown (ref 1)]

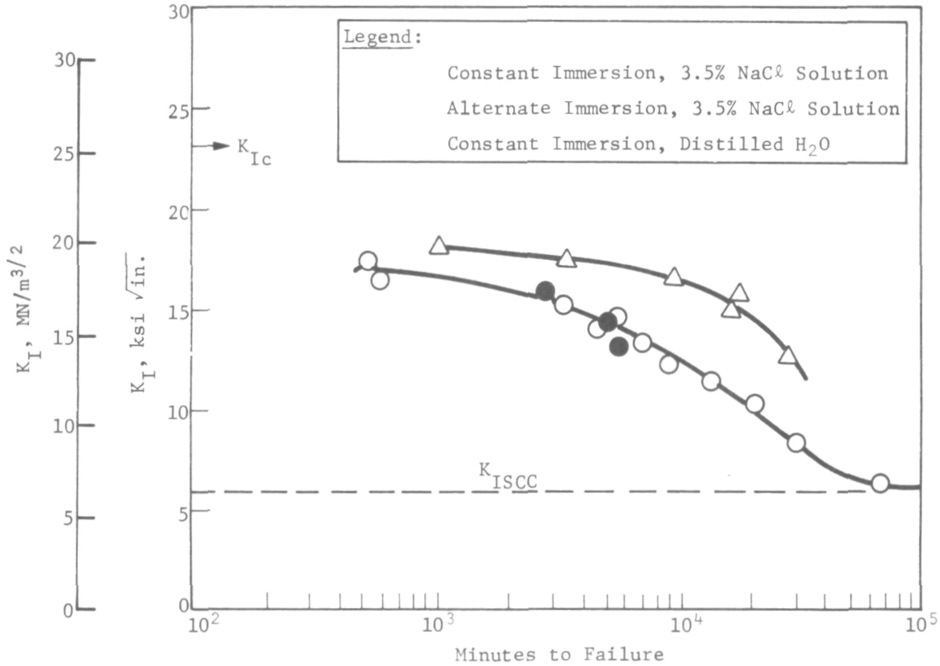

Figure 2.- Stress corrosion data for 7075-T6 Aluminum (precracked specimens) [J. Mulherin (ref 3)]

The program was intended to provide data needed for reusable space vehicle design and to develop an understanding of apparent discrepancies between smooth and precracked specimen behavior. The discrepancies result from the observation that σ_{TH} values are lower than allowable stress obtained from precracked specimens with short crack lengths.

The objective of the program was to determine the sustained load stress-corrosion cracking threshold for alloy 2124 using smooth $\left(\sigma_{TH}\right)$ and precracked $\left(K_{ISCC}\right)$ specimens and the cyclic-load growth behavior in 3.5% NaCℓ salt solution. The relationship between K_{ISCC} and σ_{TH} was also to be studied.

PROGRAM PLAN

The program consisted of six tasks:

Task I - Material characterization;

Task II - Static fracture toughness tests;

Task III - Static environmental tests;

Task IV - Cyclic-load environmental tests;

Task V - Data analysis;

Task VI - Reporting.

The following paragraphs summarize the activities associated with the first four tasks.

Task I - Material Characterization

Characterization of the 5.1-cm (2-in.) thick 2124-T851 plate stock was achieved by a combination of chemical analysis (to ensure adherence to applicable specifications), metallographic examination (to determine microstructure, condition, and grain size), and mechanical property tests of the base metal to provide strength, ductility, and elasticity data.

Task II - Static Fracture Toughness Tests

Static fracture toughness of 2124 aluminum in all orientations was characterized using both surface-flaw (SF) and compact specimens (CT). Surface-flaw specimens, 1.3-cm (0.5-in.) thick, were evaluated in the longitudinal and transverse directions. Compact specimens, 1.3-cm (0.5-in.) thick, were prepared in both crack orientations of each of the three plate grain orientations for a total of six directions. Duplicate specimens were evaluated for each specimen condition.

Task III - Static Environmental Tests

The stress corrosion threshold of 2124 aluminum alloy was determined under conditions of alternate immersion using longitudinal and long transverse surface-flaw specimens, six orientations of bolt-loaded modified compact specimens, and three orientations of smooth bend specimens. As a result of data developed during the program, additional specimen types were evaluated. Short transverse surface-flaw and center-notch (CN) specimens, deadweight-loaded compact specimens, and deadweight loaded, unnotched, short transverse specimens were also tested.

Task IV - Cyclic Load Environmental Tests

The effect of the environment was evaluated by conducting a series of cyclic flaw extension tests in ambient air and a series in 3.5% NaCℓ. Both surface flawed and compact specimens were included in this series. Two directions for the surface flaw and six for the compact specimens were evaluated. All specimens were 1.3-cm (0.5-in.) thick.

EXPERIMENTAL PROCEDURES

This section describes the specimen design and preparation, instrumentation, and experimental procedures used in the program.

Specimen Design

All tensile specimens were of the round bar configuration in accordance with ASTM E8 specifications. For the longitudinal (L) and long transverse (LT) directions, the standard 1.28-cm (0.505-in.) diameter configuration was used. The short transverse (S) specimen utilized the subsize proportioned geometry with a 3.2-mm (0.125-in.) gage diameter and a 1.9-cm (0.75-in.) reduced section.

Figure 3 gives the specifications of the compact specimen with provision for bolt loading. The compact specimen was designed for either bolt or pin loading. The configuration is of standard proportions for height, width, and crack length. Thickness was reduced to 1.27 cm (0.5 in.). The rationale behind this selection was a desire to maximize the size of the specimen for ease of preparation, but to maintain the service gage thickness.

Specifications for the surface-flaw specimen used for L and LT testing are given in figure 4. The gage thickness of 1.27 cm (0.5 in.) was maintained; specimen width was 7.62 cm (3 in.).

Smooth bend specimens were designed for four-point loading. For the longitudinal and long transverse directions, a 12.7-cm (5-in.) long beam 1.9-cm (0.75-in.) wide and 3.2-mm thick (0.125-in.) was used. For the short transverse direction, the specimen was 5.04-cm (2-in.) long by 9.5-mm (0.375-in.) wide by 1.6-mm (0.062-in.) thick.

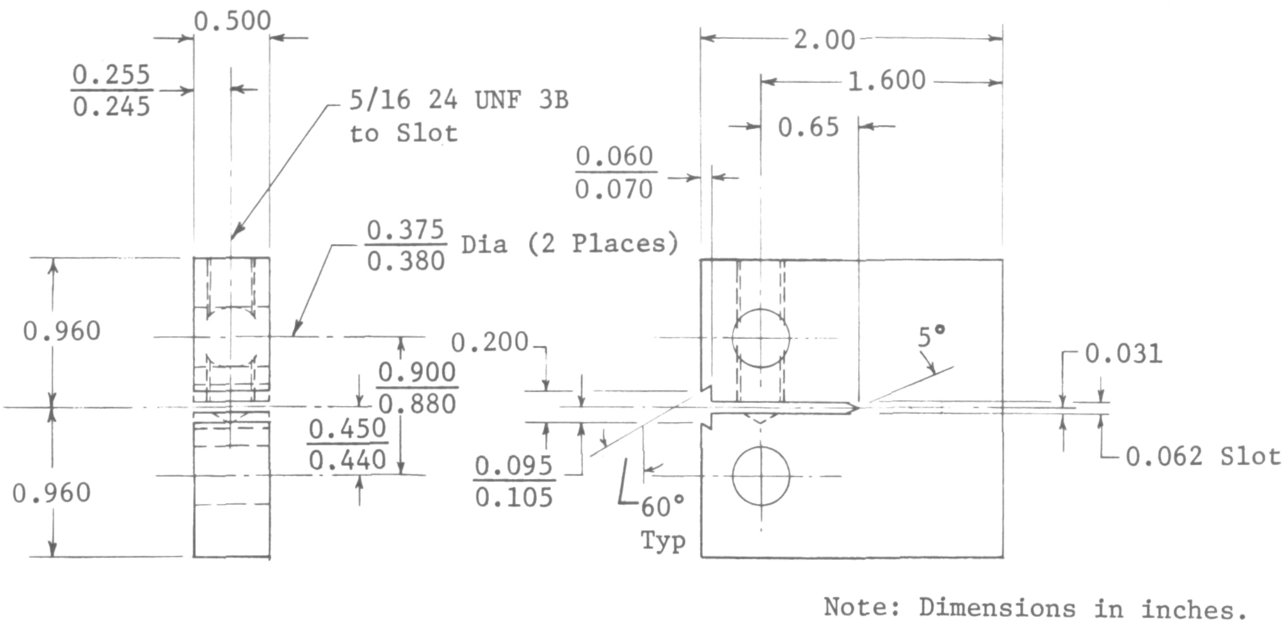

Figure 3.- Bolt-loaded compact specimen

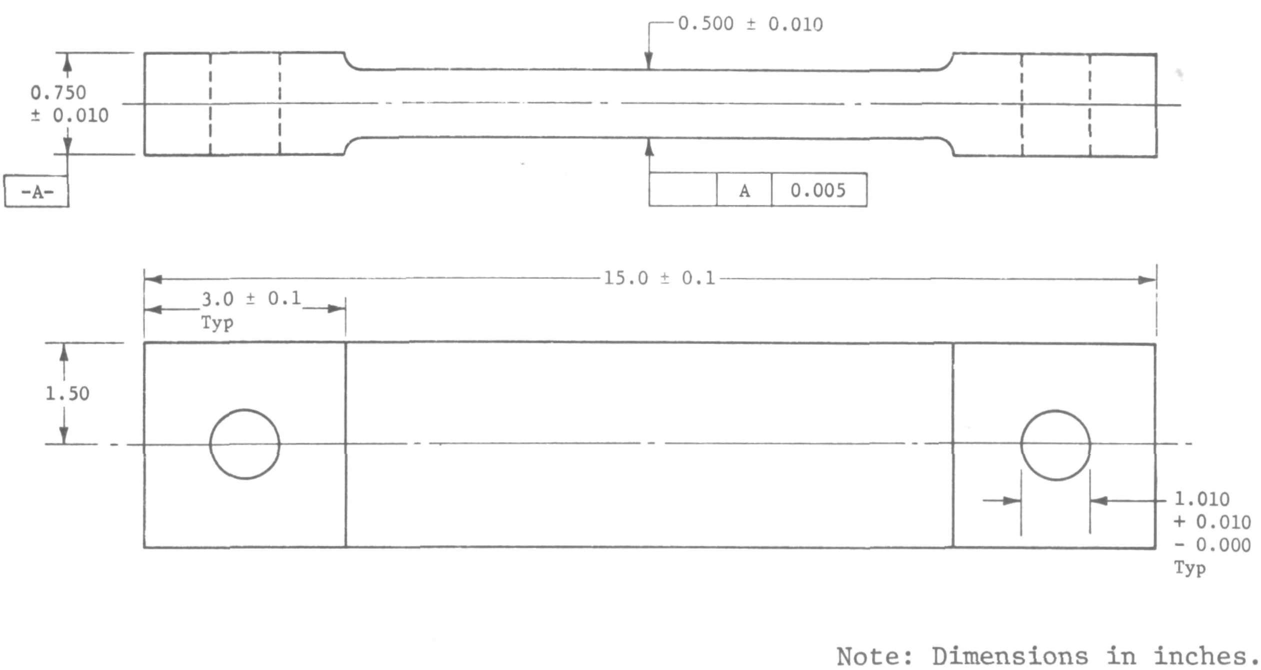

Figure 4.- Geometry for surface-flaw specimen

Additional configurations evaluated in the static stress corrosion task included uniaxial-loaded unnotched specimens and short transverse axial-loaded flawed specimens.

Figure 5 shows a uniaxial pin-loaded smooth specimen after test. The gage section was 1.9-cm (0.75-in.) wide by approximately 1.27-cm (0.50-in.) long. Gage thickness was approximately 3 mm (1/8 in.); thickness was varied so multiple specimens could be deadweight-loaded with a uniform weight to provide different stress levels.

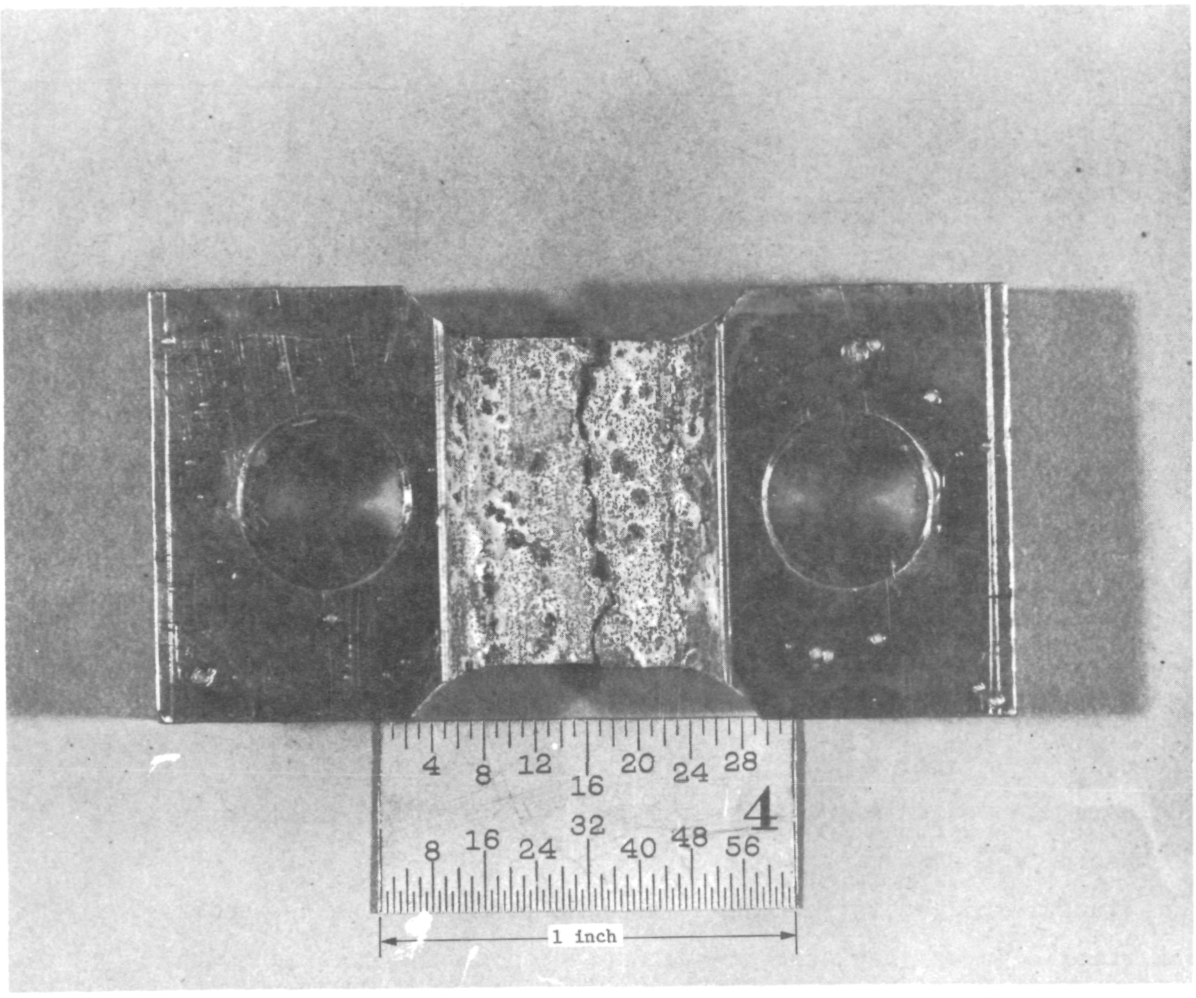

Figure 5.- Uniaxial smooth stress corrosion specimen

The short transversc axial-loaded flawed specimens were prepared by electron-beam welding extensions to a 1.27-cm (0.5-in.)

thick by 7.62-cm (3-in.) wide slab of plate stock or by maching a short transverse section for shoulder loading. Figure 6 shows a typical shoulder-loaded specimen and the grip plates used to permit pin loading the specimen assembly.

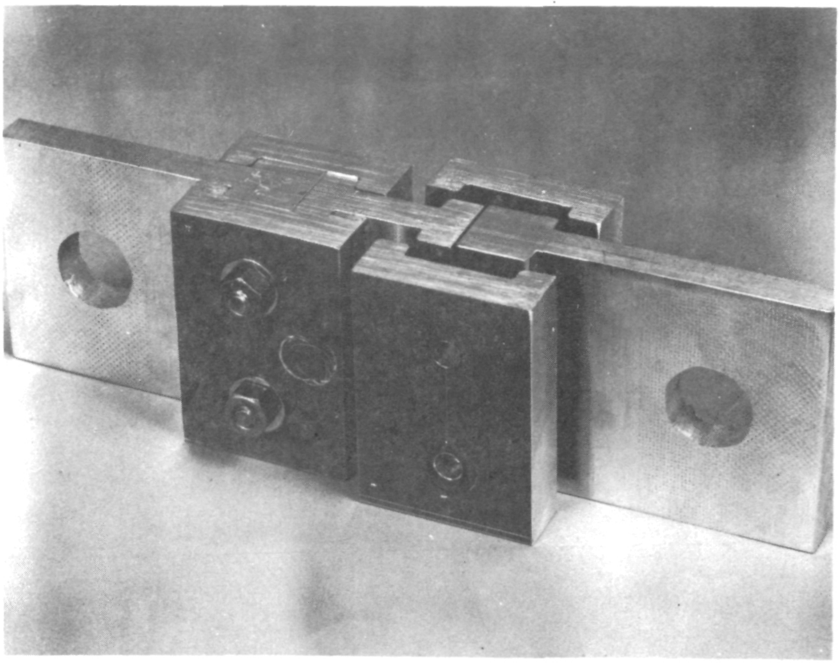

Figure 6.- Shoulder-loaded short transverse stress corrosion specimen

Instrumentation

Tensile specimens were instrumented with resistance strain gages bonded in the axial direction to provide modulus of elasticity and yield strength data. Double gages, diametrically opposed, were used to determine bending effects. The longitudinal specimens were also gaged with transverse gages to provide Poisson's ratio data.

Fracture toughness specimens were instrumented with a standard commercial clip-on displacement gage attached to the specimen with knife edges, as shown in figure 7. For bolt-loaded stress-corrosion testing and cyclic loading in air, a shorter gage-length clip-on gage was used. Figure 8 shows the gage installed on a specimen containing integral knife edges. For cyclic testing in salt water, a submersible clip gage was used. Figure 9 shows this unit.

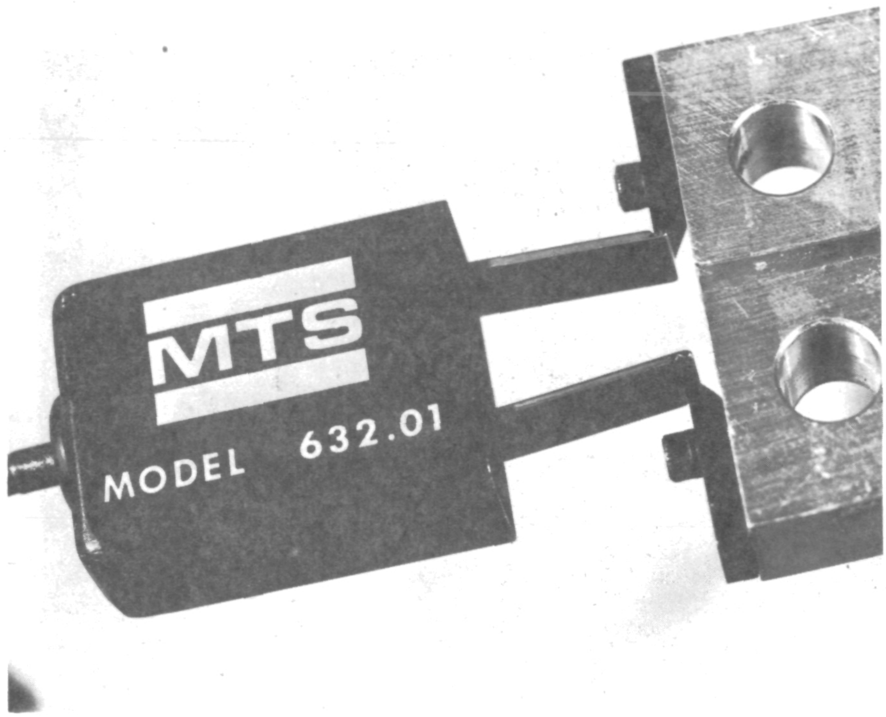

Figure 7.- Clip-on displacement gage attached to fracture toughness specimen

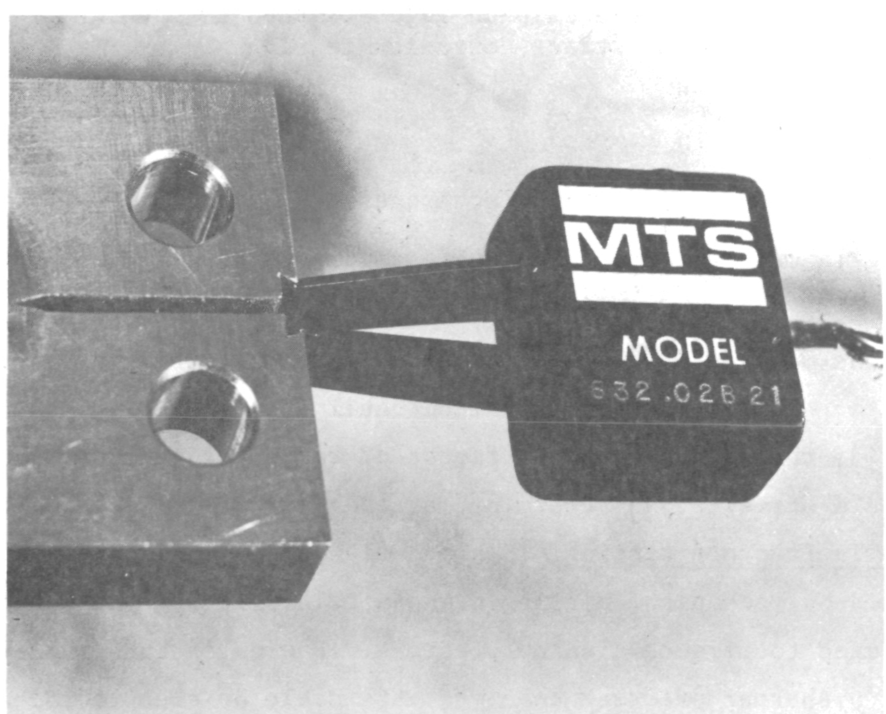

Figure 8.- Clip-on gage attached to cyclic specimen containing integral knife edges

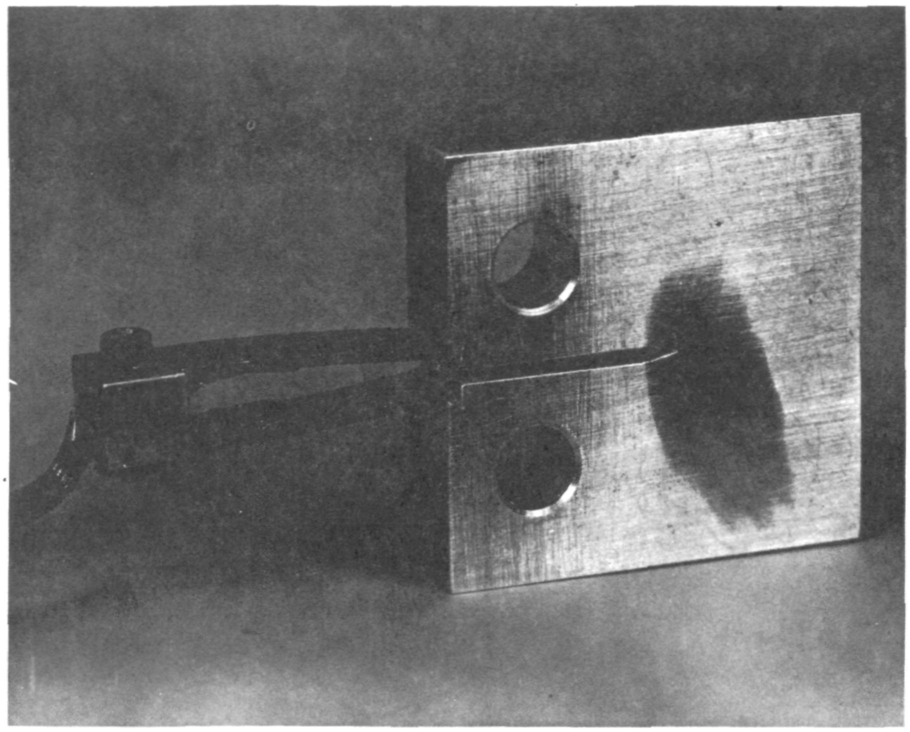

Figure 9.- Submersible clip-on gage attached to specimen used for stress corrosion testing

Testing Techniques

Tensile Testing.- Tensile testing was performed in accordance with ATM specification E8. The rate of head separation during testing was 0.25 mm (0.01 in.) per 2.54 cm (1 in.) of gage length per minute. This rate was maintained until the yield strength was determined, then increased by a factor of ten until failure occurred. Yield strength was determined by the 0.2% offset method.

Static fracture testing.- Surface-flaw specimen defects were introduced by mechanical milling using a thin slitting saw specially sharpened to produce a sharp precrack. Sawing in this manner produced a sharper precrack than was attainable by electrodischarge machining. As a result, cracking can be initiated in fewer cycles or at a lower stress. The flaw was then sharpened by fatigue extending [minimum of 1.3 mm (0.05 in.)] in tension in a closed-loop testing machine at a stress level of approximately 96 MN/m^2 (14 ksi) to produce a final depth of approximately 0.5 cm (0.2 in.) and a shape factor of slightly less than 0.3.

Compact specimens were fatigure cracked at a maximum stress intensity of 8 $MN/m^{3/2}$ (7 ksi $\sqrt{in.}$) to give a minimum crack extension of 1.3 mm (0.05 in.).

Fracture testing was performed at a loading rate of approximately 22.2 kN/min (5000 lb/min).

Stress corrosion testing.- For smooth SCC testing, both four-point loaded bent beams and uniaxial pin-loaded specimens were used.

Beam specimens were evaluated in the following manner. Center span deflection was measured and used to stress the beam to a predetermined level according to the following relationship:

$$\text{Deflection (max)} = \frac{\sigma}{3Et}\left(3/4\ \ell^2 - a^2\right)$$

where

σ = outer fiber stress

a = distance from load point to support

t = specimen thickness

E = elastic modulus

ℓ = length between end supports

The above deflection formula was verified by deflecting specimens instrumented with a strain gage on the tension surface.

The specimens were wet-sanded to remove the machined finish, loaded in the stressing frames to specified stresses (two specimens per stress level), and immediately placed in the testing environment. The loading areas of the specimens were covered with either kapton or mylar tape and the frames dipped in chem-mill masking agent to prevent dissimilar metal contact and corrosion of the test frames.

The salt solution was reagent-grade NaCℓ (sodium chloride) and deionized water. Specific gravity for a 3.5% NaCℓ solution is 1.023, and this was monitored as the test progressed. Evaporation losses were compensated for by addition of deionized water. The solution was contained in a polyethylene tub to further minimize contamination.

The alternate immersion cycle consisted of 50 minutes in solution and 10 minutes out. A pneumatic actuator was used to lower and raise the specimen rack in and out of the salt solution. The immersion cycle was controlled by an electric timer and solenoid valve.

Periodic observations were performed while the tests were in progress. At completion of the one-month testing period, all specimens were removed for detailed visual examination. Selected samples were also sectioned and examined.

Bolt-loaded compact specimens for SCC were prepared in a manner similar to that used for compact static fracture toughness specimens. The specimens were precracked a minimum of 1.3 mm (0.50 in.) in a closed-loop test machine. Precracking stress intensity was always lower than bolt-loaded values for the immersion tests.

Before the specimens were bolt-loaded, each was briefly cycled in the test machine to work the salt solution into the fatigue precrack. Bolt loading took place immediately using a stainless-steel bolt and the commercial clip-on displacement gage to determine the initial compliance value. A 6.4-mm (1/4-in.) diameter steel ball was placed between the bolt end and the specimen to ensure accurate loading. The portion of the specimen containing the bolt was dipped in molten paraffin to completely mask dissimilar metal interfaces. Figure 10 shows a typical specimen after a 30-day exposure. Note that the region surrounding the crack tip has been polished to permit crack length measurement.

The testing environment for bolt-loaded specimens was the same as that for smooth bend specimens. The alternate immersion cycle was also the same as that used for tests run with the smooth bend specimens. Periodic inspections were also made.

Posttest examination involved unloading the specimens with the clip-on gage installed to determine the amount of crack opening maintained. Compliance was measured by loading statically in the test machine. The specimens were then fatigue-marked and fractured or sectioned for metallographic examination.

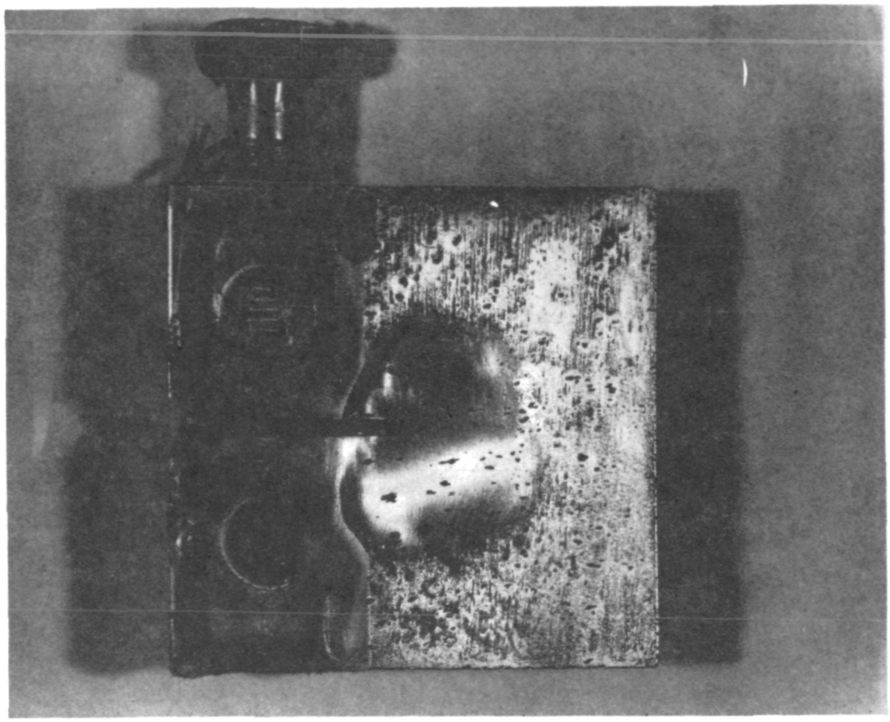

Figure 10.- Typical bolt-loaded compact specimen after 30-day stress corrosion exposure

The uniaxial pin-loaded type of specimen was stressed in a creep rack using deadweight loading. The requirement for alternate immersion exposure required a rather unique scheme for environmental cycling. The common system used for nonloaded or fixture-loaded specimens cannot be used for specimens installed in creep racks. For this work, a system that pumped the environment into plastic containers surrounding the specimens for a 10-minute period and then emptied the container for a 50-minute period was developed. The system, shown schematically in figure 11, consisted of a supply reservoir pressurized by a pump to fill the environmental container. A float-operated switch was used to close a solenoid-operated valve between the container and reservoir and to stop the pump and vent the reservoir.

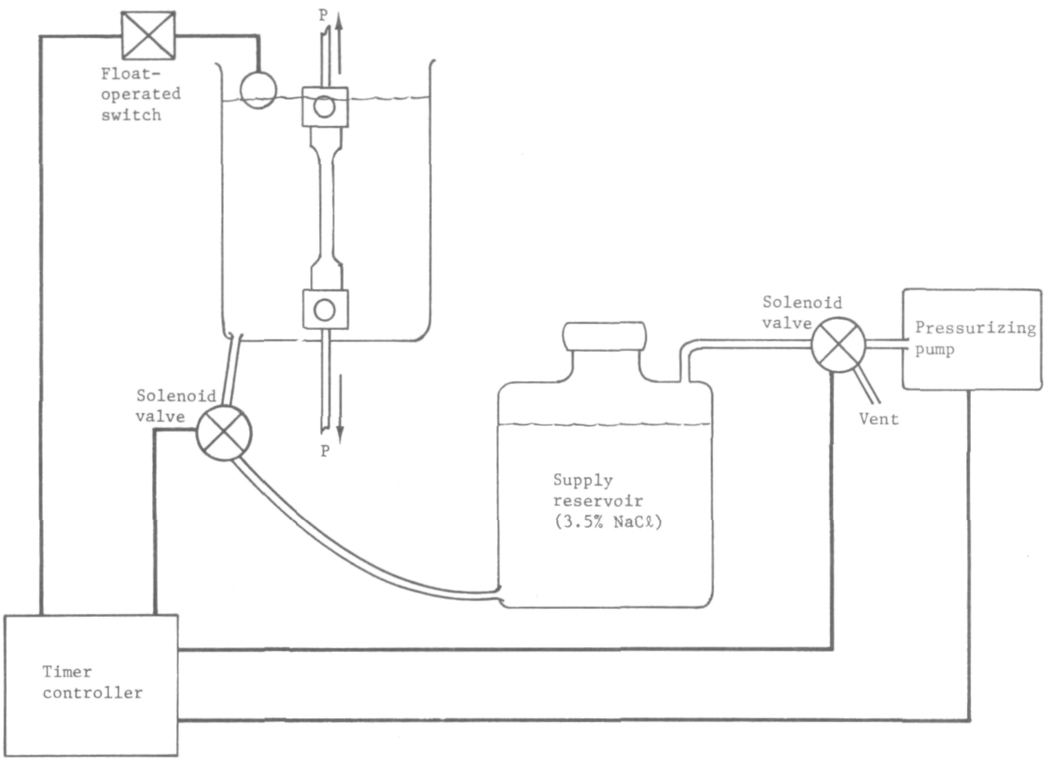

Figure 11.- Schematic diagram for environmental control system

After 10 minutes, the solenoid valve between the container and reservoir opened and gravity drained the liquid back to the supply container. A number of containers were operated simultaneously from a single reservoir by manifolding additional supply lines and solenoid valves. Figure 12 shows a composite view in which three creep racks are equipped with alternate immersion containers.

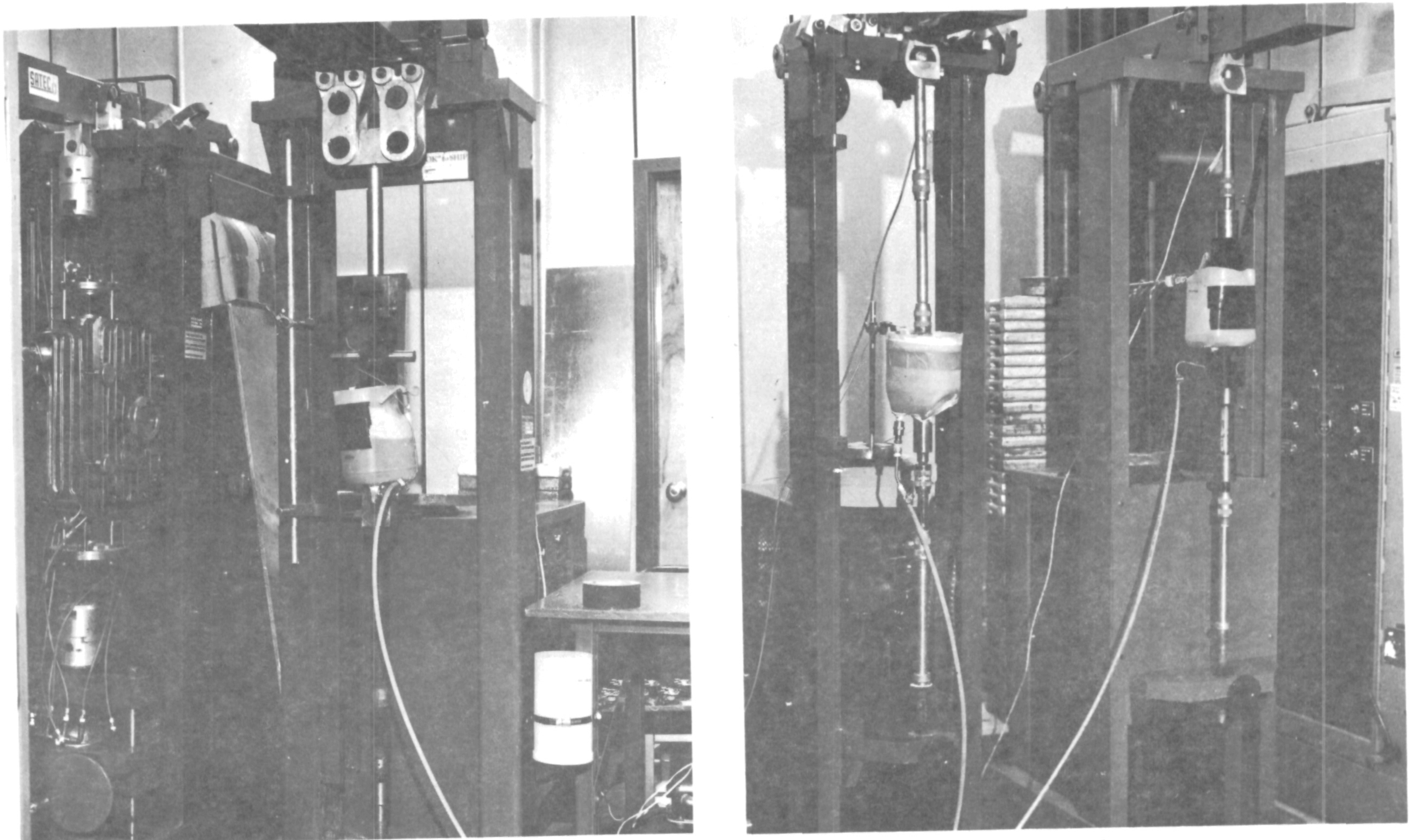

Figure 12.- View of creep racks with alternate immersion containers

Cyclic crack growth tests.- Cyclic crack growth tests were performed using both compact and surface-flaw specimens in air and 3.5% NaCℓ solution.

The compact specimen tests when performed in air were conducted using the commercial clip-on displacement gage. A compliance curve was obtained by scribing the two surfaces at the end of the crack and obtaining crack-opening displacement readings. The submersible compliance gage characteristics are identical to those of the gage used for testing in air. Therefore, compliance data obtained during performance of the testing in air permitted the environmental cyclic testing to be performed by periodically interrupting the test to obtain a compliance curve, but not requiring removal of the specimen from the container to mark the surfaces.

Surface-flaw cyclic tests were conducted to provide two or three growth bands per test. Staining with a 10% NaOH (sodium hydroxide) solution was used to differentiate the growth bands.

EXPERIMENT RESULTS

Task I - Material Characterization

This task was performed to provide mechanical property characterization to assure adherence to specifications and to provide baseline data. The following test were included in this task:

1) Chemical analysis;
2) Metallographic examination;
3) Tensile property determination.

The 2124-T851 aluminum alloy was procured as a single plate, 122 cm (48 in.) x 244 cm (96 in.) x 5.1 cm (2 in.), from McDonnell Douglas, St. Louis, Missouri. No test reports or certification data were obtained.

Chemical analysis showed that the composition met the 2124 specification limits. The comparative data are as follows:

Element, weight %	Si	Fe	Cu	Mn	Mg	Zn
Specification	0.20	0.30	3.8 - 4.9	0.3 - 0.9	1.2 - 1.8	0.25
Martin Marietta analysis	0.08	0.12	3.8	0.7	1.4	0.01

Metallographic examination of the 2124-T851 alloy plate revealed evidence of overheating during processing. The structure was on the verge of incipient melting as shown by agglomeration of second-phase particles. The grain size was very coarse. Photomicrographs showing the three grain orientations are presented in figures 13 through 15.

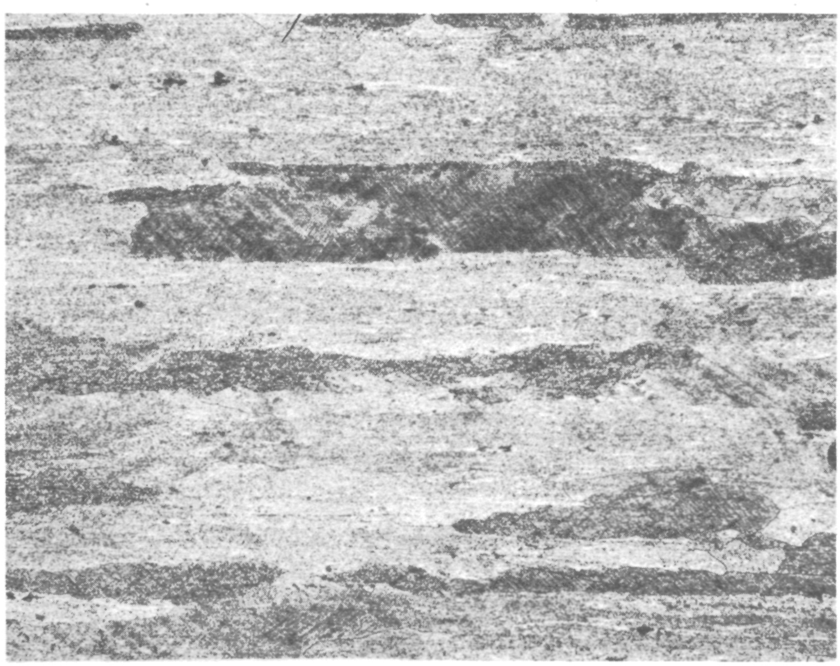

Etchant: Keller's 100X

Figure 13.- Microstructure of 2124-T851 plate (perpendicular to longitudinal direction)

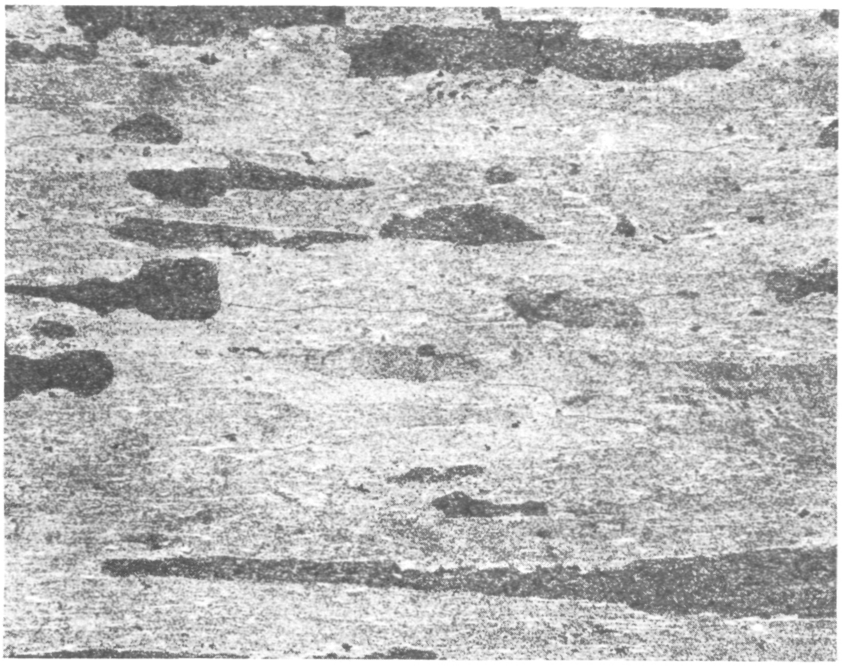

Etchant: Keller's 100X

Figure 14.- Microstructure of 2124-T851 plate (perpendicular to transverse direction)

Etchant: Keller's 50X

Figure 15.- Microstructure of 2124-T851 plate (perpendicular to short transverse direction)

A sample of the plate stock was metallographically examined by an aluminum producer. He reported that, although the material exhibited agglomeration and coarse grain size, it was typical of commercial practice and was of acceptable quality.

The grain size, as measured on an end section, was between ASTM 0 and -1. Grains measured in the rolling and edge section views were up to 10 times longer than their width.

Tensile tests were made using specimens with the loading axis parallel to the longitudinal, long tansverse, and short transverse directions. The tensile property data shown in table I were normal for 2124-T851. Elastic property data are given in table II.

TABLE I

TENSILE PROPERTIES OF 2124-T851 ALUMINUM ALLOY

Grain direction	Ultimate strength, MN/m^2 (ksi)	Yield strength, MN/m^2 (ksi)	Elongation, %	Reduction in area, %
Longitudinal (L)	494 (71.6) 497 (72.0)	452 (65.6) 454 (65.8)	10 Avg	23 18
	496 (71.8) Avg	453 (65.6) Avg		20 Avg
Long transverse (LT)	498 (72.2) 494 (71.6)	452 (65.5) 452 (65.5)	8 8	14 18
	496 (71.9) Avg	452 (65.5) Avg	8 Avg	16 Avg
Short transverse (ST)	462 (67.0) 462 (67.0)	422 (61.2) 420 (60.8)	4 3	1 1
	462 (67.0) Avg	421 (61.0) Avg	4 Avg	1 Avg

TABLE II

ELASTIC PROPERTIES OF 2124-T851 ALUMINUM ALLOY

Loading direction	Poisson's ratio	Modulus of elasticity, MN/m^2 (10^6 psi)
Longitudinal (L)	0.327	72.9×10^3 (10.56)
	0.334	72.5 (10.50)
	0.330 Avg	72.7 (10.53) Avg
Long Transverse (LT)	--	72.9×10^3 (10.56)
		73.3 (10.63)
		73.1 (10.60) Avg
Short Transverse (ST)	--	68.2×10^3 (9.89)
		70.6 (10.23)
		69.4 (10.06) Avg

Task II - Static Fracture Toughness Tests

Static fracture toughness data were obtained using both surface flaw (SF) and compact (CT) specimens.

The surface flaw tests in the longitudinal (LS) and long transverse (TS) directions exhibited failure at between 80 and 90 percent of the yield strength. The letter code (i.e., LS, TS) above refers to the direction of loading and crack orientation direction as shown in figure 16 for both the surface-flaw and compact types of specimens. Fracture face examination revealed evidence of delamination at the crack periphery. A single test performed in the short longitudinal soecimen (figure 16) with transverse crack orientation (LT) also exhibited a high fracture stress but no evidence of delamination.

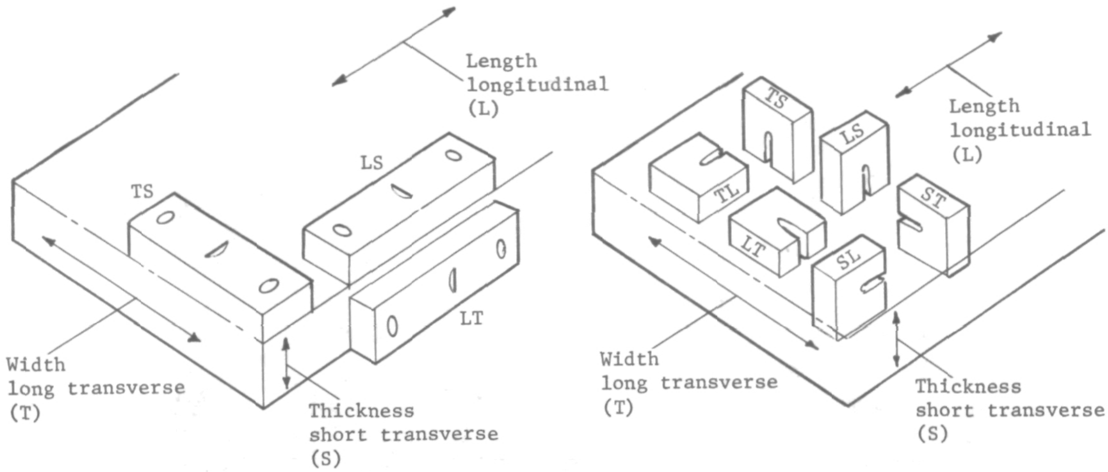

Figure 16.- Specimen direction identification system

Toughness data are summarized in table III. Typical fracture face photos are given in figures 17 through 19.

TABLE III

FRACTURE PROPERTIES OF 2124-T851 ALUMINUM ALLOY
(Surface Flaw Specimen)

Specimen orientation	Crack size			Fracture stress, MN/m^2 (ksi)	σ_f/σ_y	Static fracture toughness, $MN/m^{3/2}$ (ksi $\sqrt{in.}$)
	a, mm (in.)	2C, mm (in.)	a/2C			
Longitudinal (LS)	5.13 (0.202) 5.13 (0.202)	18.2 (0.715) 18.2 (0.715)	0.283 0.283	403 (58.5) 407 (59.0)	0.89 0.90	47.5* (43.2)* 48.0* (43.7)* 47.8 (43.5) Avg
Transverse (TS)	5.38 (0.212) 5.08 (0.200)	18.3 (0.719) 18.7 (0.718)	0.295 0.279	372 (54.0) 395 (57.3)	0.82 0.88	44.0* (40.0)* 46.4* (42.2)* 45.7 (41.1) Avg
Short longitudinal (LT)	4.72 (0.186)	15.7 (0.620)	0.300	381 (55.3	0.90	42.2 (38.4) Avg

*Specimens delaminated at crack front; data invalid.

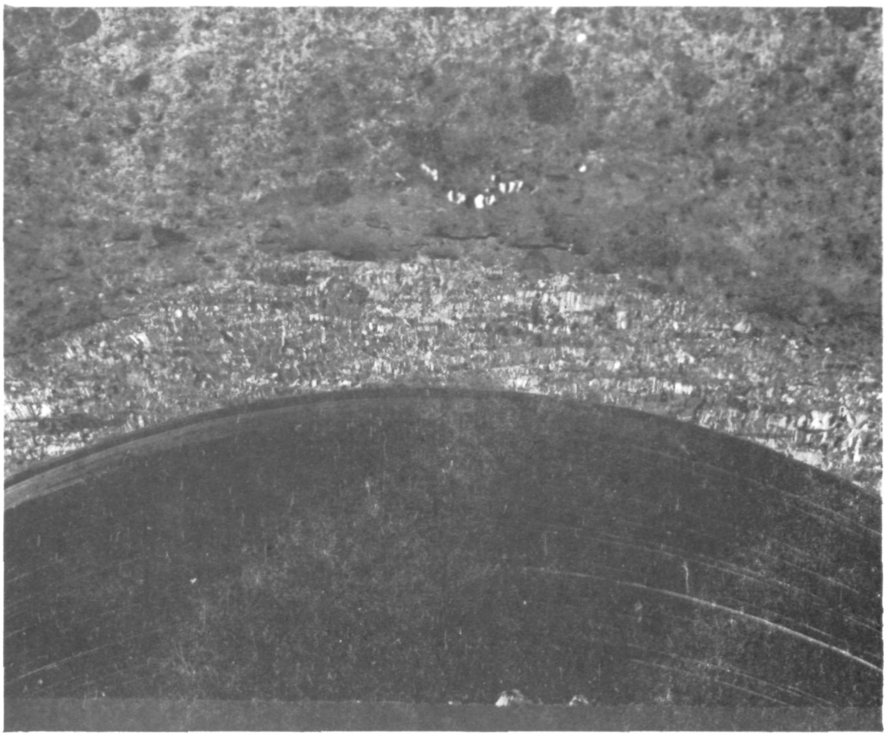

Mag. 12X

Figure 17.- Fracture face of longitudinal surface flaw specimen (LS orientation) showing delaminations near crack front

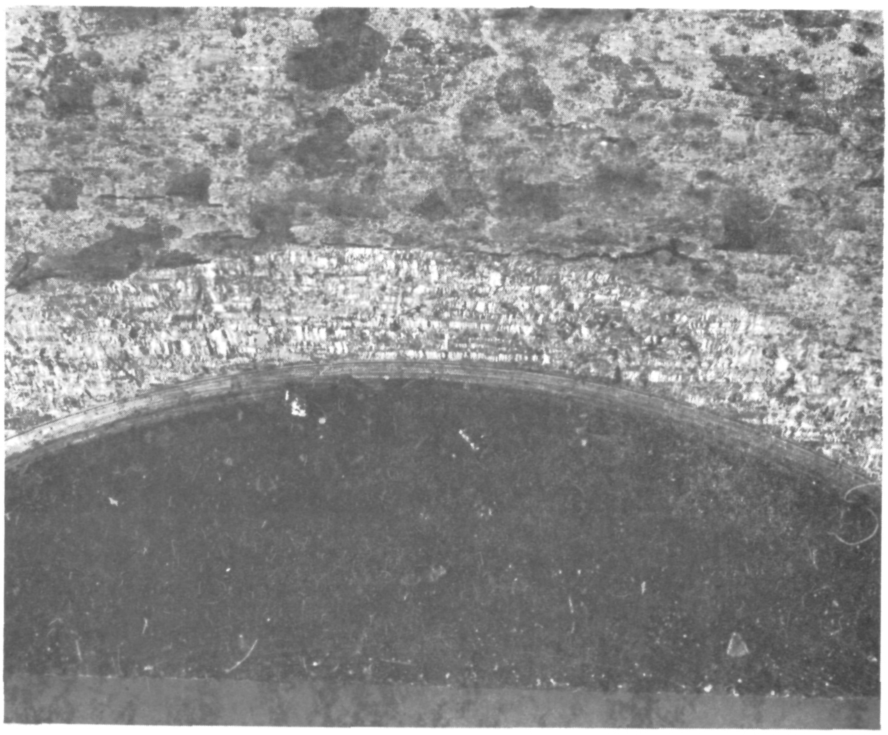

Mag. 12X

Figure 18.- Fracture face of transverse surface flaw specimen (TS orientation) showing delaminations near crack front

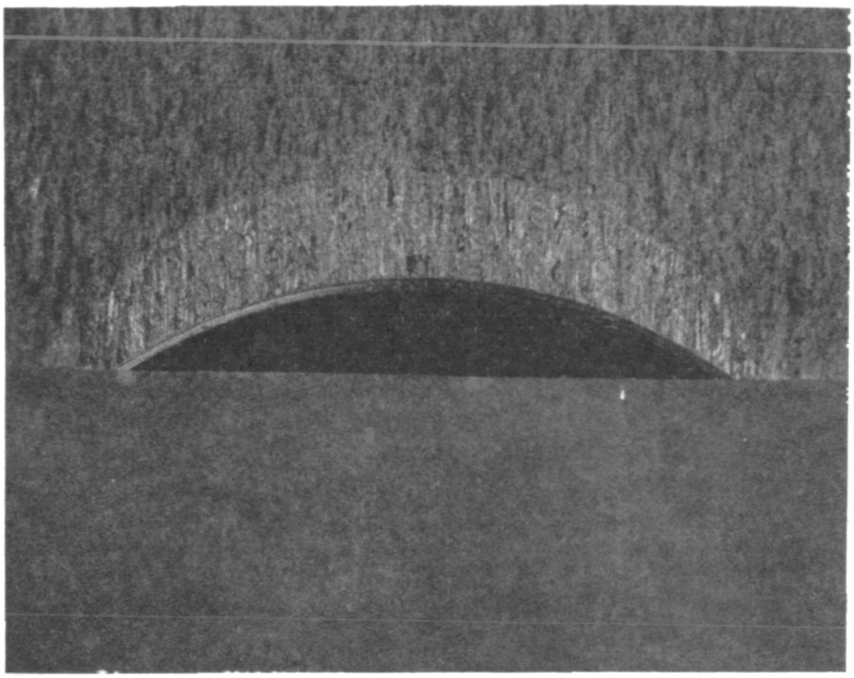

Mag. 6X

Figure 19.- Fracture face of longitudinal surface flaw specimen (LT orientation)

The compact specimen data are given in table IV. The LS and LT specimens failed out of plane; fracture progressed at a large angle with respect to the crack axis (figure 20). Toughness values for the other directions varied from approximately 24 to 32 $MN/m^{3/2}$ (22 to 29 ksi $\sqrt{in.}$). The lowest toughness readings were for the SL and ST orientations. Figure 21 shows a typical fracture face for each orientation.

TABLE IV

FRACTURE PROPERTIES OF 2124-T851 ALUMINUM ALLOY (CT SPECIMEN)*

Specimen orientation	Load		P_{max}/P_Q	K_Q, $MN/m^{3/2}$ (ksi $\sqrt{in.}$)	$(K_Q/\sigma_{ys})^{2}$ †	K_{Ic}, $MN/m^{3/2}$ (ksi $\sqrt{in.}$)
	P_Q, kN (kips)	P_{max}, kN (kips)				
LT	8.23 (1.85) 8.68 (1.95)	9.21 (2.07) 9.52 (2.14)	1.12 1.10	30.8 (28.0) 32.4 (29.5)	0.46 0.50	30.8 (28.0) 32.4 (29.5) 31.6 (28.8) Avg
TL	7.57 (1.70) 7.78 (1.75)	7.78 (1.75) 8.10 (1.82)	1.03 1.04	28.2 (25.7) 29.0 (26.4)	0.38 0.41	28.2 (25.7) 29.0 (26.6) 28.6 (26.0) Avg
LS	10.23 (2.30) 9.56 (2.15)	10.94 (2.46) 10.54 (2.37)	1.07 1.10	38.2 (34.8) 35.7 (3 .5)	0.70 0.61	¶ ¶ ¶ ¶
TS	9.43 (2.12) 8.90 (2.00)	10.10 (2.27) 9.74 (2.19)	1.07 1.09	35.3 (32.1) 33.2 (30.2)	0.60 0.53	¶ ¶ ¶ ¶
SL	6.36 (1.43) 6.72 (1.51)	6.36 (1.43) 6.72 (1.51)	1.00 1.04	23.6 (21.5) 24.1 (21.9)	0.31 0.32	23.6 (21.5) 24.1 (21.9) 23.8 (21.7) Avg
ST	6.67 (1.50) 6.18 (1.39)	6.89 (1.55) 6.32 (1.42)	1.03 1.02	24.9 (22.7) 23.1 (21.0)	0.35 0.30	24.9 (22.7) 23.1 (21.0) 24.0 (21.8) Avg

*Crack length, a = 2 cm (0.8 in.), a/W = 0.50, Y = 9.6.

†σ_{ys} longitudinal = 452 MN/m^2 (65.6 ksi),
transverse = 451 MN/m^2 (65.5 ksi),
short transverse = 420 MN/m^2 (61.0 ksi).

¶Specimen failed out of plane.

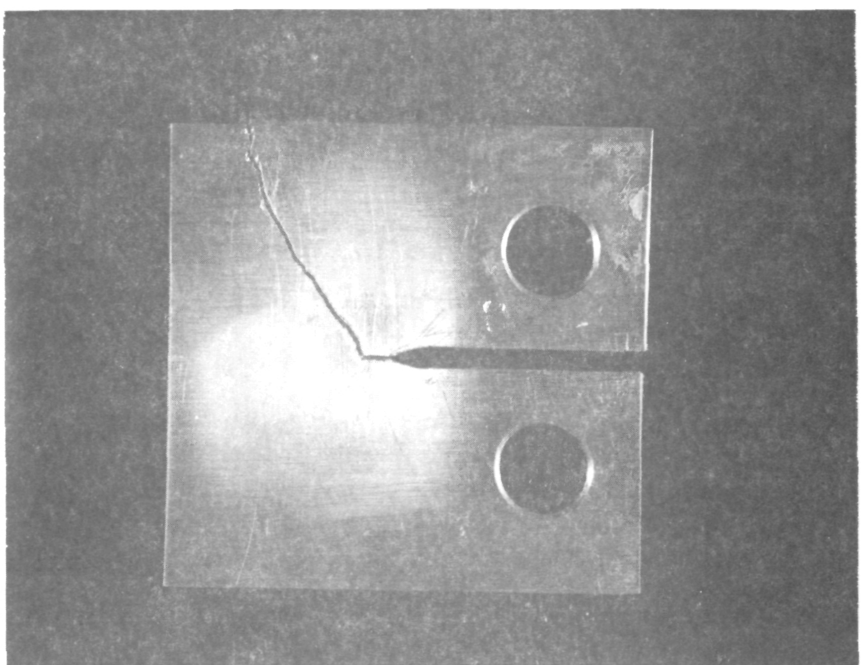

Figure 20.- View of out-of-plane fracture

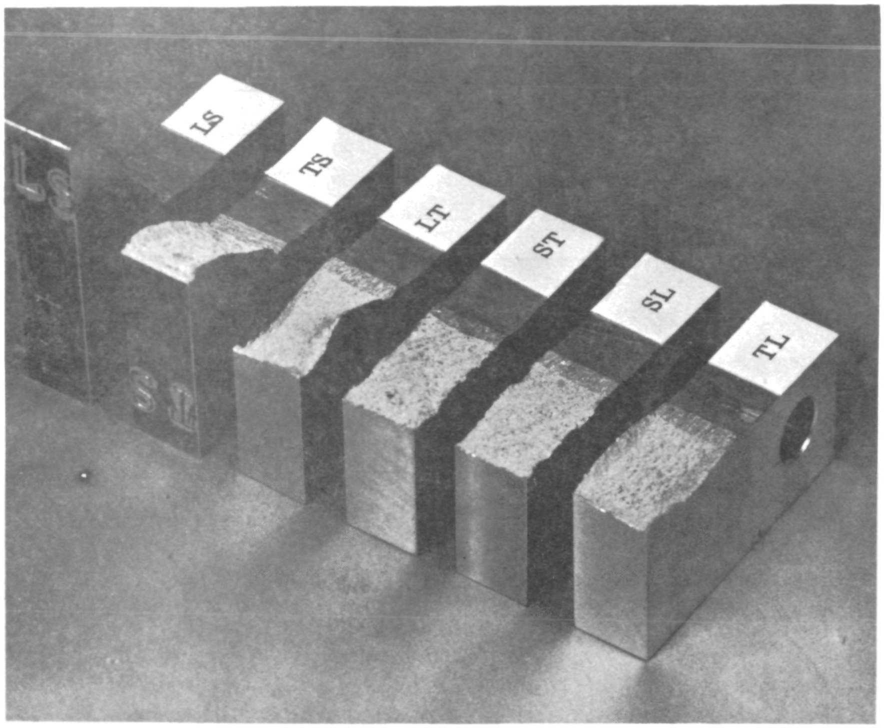

Figure 21.- Fracture faces for compact specimens

Task III - Static Environmental Tests

This task included evaluation of both smooth stress-corrosion specimens and precracked fracture-mechanics-type specimens.

Unnotched stress corrosion tests.- One-month alternate immersion tests were performed using smooth bend specimens. Stress levels were 207 (30), 276 (40), 344 (50), and 413 MN/m^2 (60 ksi). All longitudinal and long transverse specimens survived exposure without failures. Metallographic examination revealed surface pitting and general corrosion, but no evidence of stress corrosion cracking. Table V summarizes the data and shows the location of each specimen with respect to plate thickness.

Specimens tested in the short transverse direction exhibited stress corrosion cracking (table VI). Tests conducted at 276 MN/m^2 (40 ksi) exhibited shallow [0.05-mm (0.02-in.)] intergranular cracks after 30-day exposure. Specimens tested at 344 MN/m^2 (50 ksi) exhibited cracking extending almost through the thickness in 10 days.

TABLE V

ALTERNATE IMMERSION STRESS CORROSION TEST DATA FOR SMOOTH BEND SPECIMENS (LONGITUDINAL AND LONG TRANSVERSE DIRECTIONS)

Specimen orientation and location	Stress level, MN/m^2 (ksi)	Exposure period, days	Results of metallographic examination
L-4	207 (30)	30	Surface pitting and general corrosion, no SCC
L-8	207 (30)	30	
L-3	276 (40)	30	
L-7	276 (40)	30	
L-2	344 (50)	30	
L-6	344 (50)	30	
L-1	413 (60)	30	
L-5	413 (60)	30	
T-4	207 (30)	30	Surface pitting and general corrosion, no SCC
T-8	207 (30)	30	
T-3	276 (40)	30	
T-7	276 (40)	30	
T-2	344 (50)	30	
T-6	344 (50)	30	
T-1	413 (60)	30	
T-5	413 (60)	30	

Specific location with respect to plate thickness:

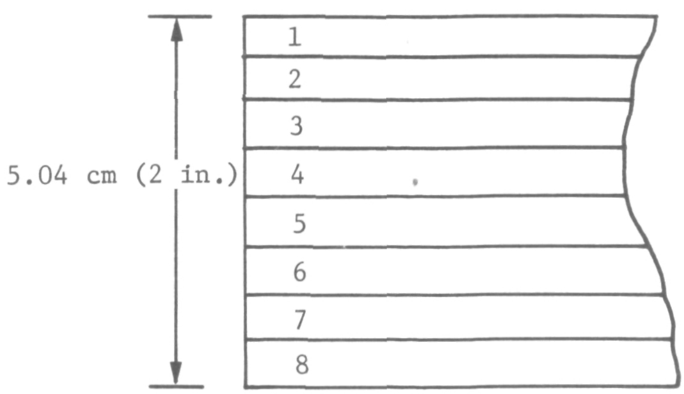

TABLE VI

ALTERNATE IMMERSION STRESS CORROSION TEST DATA
FOR SMOOTH BEND SPECIMENS (SHORT TRANSVERSE DIRECTION)

Orientation	Stress level, MN/m^2 (ksi)	Exposure period, days	Results of metallographic inspection
ST	207 (30) 207 (30)	30 30	No cracking, surface pitting
ST	276 (40) 276 (40)	30 30	Intergranular cracks ∿ 0.05-mm (0.020-in.) long, surface pitting
ST	344 (50) 344 (50)	10 30	Pronounced cracking almost through thickness, surface pitting
ST	413 (60) 413 (60)	10 10	Very pronounced cracking
SL	207 (30) 207 (30)	30 30	No cracking, surface pitting
SL	276 (40) 276 (40)	30 30	Intergranular cracks ∿ 0.05-mm (0.020-in.) in length, surface pitting
SL	344 (50) 344 (50)	30 20	Pronounced cracking, almost through thickness, surface pitting
SL	413 (60) 413 (60)	20 10	Very pronounced cracking

A series of tests was performed using pin-loaded miniature tension specimens oriented in the SL direction. The results confirmed the data obtained in bending and permitted the threshold level to be better bracketed. Data are summarized in table VII.

TABLE VII

ALTERNATE IMMERSION STRESS CORROSION TEST DATA
FOR AXIAL-LOADED SMOOTH SPECIMENS (SHORT TRANSVERSE DIRECTION)

Stress level, MN/m^2 (ksi)	Exposure period, days	Results of examination
146 (21.2)	30	Surface pitting and general corrosion, no SCC
166 (24.1)	30	Surface pitting and general corrosion, no SCC
207 (30.0)	30	Surface pitting and general corrosion, no SCC
231 (33.5)	30	Surface pitting and general corrosion, no SCC
249 (36.1)	30	Surface pitting and general corrosion, no SCC
272 (39.5)	30	Surface pitting and general corrosion, no SCC
294 (42.6)	9	Failed, SCC
327 (47.5)	9	SCC*

*Failed during reloading after other specimen in load train failed due to SCC.

Compact-specimen stress-corrosion tests.- Bolt-loaded compact were alternate-immersion tested for 30 days in all six orientations. Specimens machined from short transverse orientations (SL and ST) were loaded to levels between 0.5 and 0.73 of K_{Ic}. The longitudinal and long transverse specimens were loaded to levels between 0.6 and 0.9 of K_{Ic}. No failures occurred during the exposure period. Compliance measurements made before and after exposure showed no evidence of crack extension. Each specimen was examined metallographically or by visual inspection of the fractured surface. No evidence of stress corrosion cracking was found. Table VIII summarizes test conditions.

TABLE VIII

TEST CONDITIONS FOR ALTERNATE IMMERSION TESTING OF BOLT-LOADED COMPACT SPECIMENS

Specimen number	a/W	Stress intensity, $MN/m^{3/2}$	(ksi $\sqrt{in.}$)	K_{Ii}/K_{Ic}
LS-1	0.549	36.2	(32.9)	0.9
LS-2	0.552	36.2	(32.9)	0.9
LS-3	0.553	32.2	(29.3)	0.8
LS-4	0.550	32.2	(29.3)	0.8
LS-5	0.554	28.1	(25.6)	0.7
LS-6	0.553	28.1	(25.6)	0.7
LS-7	0.556	24.2	(22.0)	0.6
LS-8	0.554	24.2	(22.0)	0.6
LT-1	0.555	31.4	(28.6)	0.9
LT-2	0.553	31.4	(28.6)	0.9
LT-3	0.557	27.9	(25.4)	0.8
LT-4	0.556	27.9	(25.4)	0.8
LT-5	0.556	24.5	(22.3)	0.7
LT-6	0.557	24.5	(22.3)	0.7
LT-7	0.557	21.0	(19.1)	0.6
LT-8	0.557	21.0	(10.1)	0.6
TS-1	0.550	33.3	(30.3)	0.9
TS-2	0.558	33.3	(30.3)	0.9
TS-3	0.558	29.7	(27.0)	0.8
TS-4	0.553	29.7	(27.0)	0.8
TS-5	0.558	25.9	(23.6)	0.7
TS-6	0.556	25.9	(23.6)	0.7
TS-7	0.552	22.2	(20.2)	0.6
TS-8	0.556	22.2	(20.2)	0.6
TL-1	0.556	26.8	(24.4)	0.9
TL-2	0.554	26.8	(24.4)	0.9
TL-3	0.554	23.8	(21.7)	0.8
TL-4	0.555	23.8	(21.7)	0.8
TL-5	0.552	20.9	(19.0)	0.7
TL-6	0.555	20.9	(19.0)	0.7
TL-7	0.546	17.9	(16.3)	0.6
TL-8	0.551	17.9	(16.3)	0.6
SL-3	0.544	16.5	(15.0)	0.7
SL-8	0.530	16.5	(15.0)	0.7
SL-4	0.562	14.3	(13.0)	0.6
SL-7	0.539	14.3	(13.0)	0.6
SL-1	0.535	12.1	(11.0)	0.5
SL-2	0.564	12.1	(11.0)	0.5
SL-5	0.530	9.9	(9.0)	0.41
SL-6	0.524	9.9	(9.0)	0.41
ST-2	0.696	17.6	(16.0)	0.73
ST-8	0.484	17.6	(16.0)	0.73
ST-1	0.559	14.3	(13.0)	0.6
ST-7	0.557	14.3	(13.0)	0.6
ST-3	0.538	12.1	(11.0)	0.5
ST-4	0.556	12.1	(11.0)	0.5
ST-5	0.529	9.9	(9.0)	0.41
ST-6	0.529	8.8	(8.0)	0.36

To confirm the experimental results obtained from bolt-loaded test specimens, several short transverse specimens were deadweight-loaded at high percentages of K_{Ic} for 30 days. No failures or evidence of stress-corrosion attack were found. Specimens SL-17 and SL-18 were evaluated with short cracks (a/W < 0.3) to maximize the load level required. Stress intensity levels were as tabulated.

Specimen number	a/W	Stress intensity $MN/m^{3/2}$	Stress intensity (ksi $\sqrt{in.}$)	Ki/K_{Ic}
S1-16	0.618	15.8	14.4	0.65
SL-17	0.296	17.7	16.1	0.74
SL-18	0.298	17.7	16.1	0.74
SL-17	0.298	20.8	18.9	0.87
SL-18	0.300	20.8	18.9	0.87
ST-15	0.643	17.7	16.1	0.75
ST-12	0.665	19.7	17.9	0.82

Surface-flaw stress-corrosion tests.- Longitudinal (LS)* and long transverse (TS)* surface-flaw specimens were alternate-immersion exposed for 30 days. After exposure, the specimens were fatigue-marked and fractured. Examination revealed that no SCC had occurred in any of the LS specimens. Two TS specimens showed no evidence of SCC; however, one showed a slight growth in the 2C direction, approximately 1 mm (0.04 in.) on one side only, but no growth in the depth (a) direction. Table IX summarizes the test data.

---

* Refer to figure 16.

TABLE IX

TEST CONDITIONS FOR ALTERNATE IMMERSION
TESTING OF SURFACE FLAW SPECIMENS

Specimen number	Flaw size			Stress,		Q	Stress intensity,	
	a, mm (in.)	2C, mm (in.)	a/2C	MN/m^2	(ksi)		$MN/m^{3/2}$	(ksi $\sqrt{in.}$)
L-1	4.19 (0.165)	17.0 (0.670)	0.247	227	(33)	1.40	24.2	(22.0)
L-2	8.38 (0.330)	25.6 (1.085)	0.314	227	(33)	1.59	32.2	(29.3)
L-3	5.16 (0.203)	22.9 (0.900)	0 226	227	(33)	1.34	27.5	(25.0)
T-1	4.19 (0.165)	18.0 (0.710)	0.233	227	(33)	1.36	24.6	(22.4)
T-2	8.00 (0.315)	27.5 (1.084)	0.290	227	(33)	1.54	32 0	(29 1)
T-3	5.33 (0.210)	22.2 (0.874)	0.242	227	(33)	1.39	27.5	(25.0)
LT-2A	2.95 (0.116)	15.8 (0.621)	0.187	268	(39)	1.22	25 8	(23.5)
LT-2B	4.29 (0.169)	13.5 (0.530)	0.318	268	(39)	1.39	27.1	(24.7)
LT-3A	3.12 (0.123)	16.0 (0.629)	0.195	172	(25)	1 28	16.6	(15.1)
LT-3B	5.51 (0.217)	19.1 (0.753)	0.318	172	(25)	1.55	20.1	(18.3)

As a result of the growth found in the 2C direction, two specimens were prepared in the short longitudinal direction (LT) and exposed for 30 days to determine whether growth would occur in the depth direction. Test conditions are summarized in table IX. Posttest evaluation showed no evidence of growth.

Additional tests.- The absence of stress corrosion cracking in the compact fracture specimens might be attributed to the low nominal stress inherent in this type of specimen, which uses a large crack and tensile bending to develop crack-tip stress intensity. Failure to find SCC might indicate stress below a *stress* threshold rather than a *stress intensity* threshold.

Axial loaded specimens (such as the surface flaw and center notch) typically achieve a given stress intensity level through the combination of a smaller crack size and larger stress than the compact specimen. If SCC threshold is *stress*-dependent, evaluation of alternate specimens loaded to higher stress levels than the compact type might show the effect of stress.

The problem with the use of axial-loaded specimens is that aluminum alloys generally are most susceptible to SCC in the short transverse direction, and fabrication of test specimens in this direction is difficult.

A series of short transverse (SL) surface-flaw specimens was prepared by electron-beam welding extension tabs to plate-thickness blanks. These specimens were deadweight loaded in creep racks. The data presented in table X show that all specimens exhibited SCC. Three failed during the 30-day exposure due to SCC in the weld joint; however, they also exhibited SCC extending from the surface flaw.

TABLE X

TEST RESULTS FOR ALTERNATE IMMERSION TESTING OF SHORT TRANSVERSE (SL) SURFACE FLAW SPECIMENS WITH WELDED LOADING TABS

Flaw size						
a, mm (in)	2C, mm (in)	a/2C	Stress, MN/m^2 (ksi)	Q	Stress intensity, $MN/m^{3/2}$ (ksi $\sqrt{in}$)	Comments
5 64 (0 230)	18 0 (0 736)	0 312	145 (21)	1 64	16 8 (15 3)	Fractured through weld after 3 days, defect exhibited ∿ 2 3 mm (0 09 in) uniform SCC growth
6 74 (0 275)	23 2 (0 946)	0 291	145 (21)	1 57	18 9 (17 2)	Fractured through weld after 10 days, defect exhibited nonuniform growth, up to 1 mm (0 04 in)
6 69 (0 273)	21 3 (0 870)	0 314	103 (15)	1 67	13 0 (11 8)	Exposed 30 days, SCC apparent, ∿ 1 3 mm (0 05 in) in depth, ∿ 18 mm (0 7 in) in width
7 47 (0 305)	23 9 (0 975)	0 313	123 (17 9)	1 66	16 5 (15 0)	Failed through weld after 19 days, SCC apparent, nonuniform growth
5 78 (0 236)	18 4 (0 752)	0 315	125 (18 1)	1 66	14 6 (13 3)	Exposed 30 days, SCC apparent, nonuniform growth, ∿ 1.9 mm (0 075 in) in depth
8 33 (0 340)	27 9 (1 14)	0 298	90 (13 0)	1 61	12 9 (11 7)	Failed after 30 days, SCC apparent, ∿ 3 mm (0 12 in) in depth

The observation that specimens failed in or adjacent to the weld despite the presence of a defect in the center of the specimen suggested that residual stresses might be present at the weld joint. A weld section was instrumented with strain gages, then cut to relieve residual stresses. Residual stresses were found to be present. At the mid-thickness of the plates, these stresses were tension and exhibited a magnitude of 30 to 40 MN/m^2 (5 to 6 ksi). Parent metal was similarly evaluated, and it exhibited 7 MN/m^2 (1 ksi) of residual tension stress at the mid-thickness of the plate.

The finding that residual stresses were present and possibly affecting the data resulted in a reassessment of specimen requirements. Shoulder-loaded surface-flaw specimens, free from the effects of weld residual stresses, were fabricated and tested. Two such specimens were tested for 30 days. These specimens were sufficient to bracket the threshold level. Three additional specimens containing through-thickness center notches were also prepared and avaluated. These specimens were identical to the surface-flaw type except for greater width [8.9 cm (3.5 in.) compared to 7.6 cm (3 in.) for the surface-flaw specimens]. The center-notched specimens were SCC tested and bracketed the threshold. The test data are shown in table XI.

Task IV - Cyclic Load Environmental Tests

Cyclic flaw extension tests were performed in ambient air and 3.5% NaCℓ solution using both surface-flaw and compact specimens.

Surface-flaw crack growth data are presented in figure 22 through 24. Tests were performed at 5 Hz using a minimum of four specimens to obtain each curve. Two or three growth bands were obtained for each specimen. A comparison of the effect of environment for each grain direction is given in figures 26 and 27. Data reflect growth in the depth (a) direction only. The plots show a very small increase in crack growth rates for the transverse direction in 3.5% NaCℓ and virtually no environmental effect for the longitudinal direction.

TABLE XI

SURFACE-FLAW AND CENTER-NOTCH DATA

Surface-Flaw Specimens (SL)

Flaw size								Stress, MN/m^2 (ksi)		Q	Stress intensity, $MN/m^{3/2}$ (ksi $\sqrt{in.}$)		Comments
a, mm	(in.)	2C, mm	(in.)	a/2C									
7.78	(0.306)	24.7	(0.972)	0.315				124	(18)	1.66	16.6	(15.1)	SCC nonuniform growth, 1 mm (0.04 in.) max
7.26	(0.286)	24.9	(0.988)	0.291				90	(13)	1 59	11 9	(10.8)	No SCC

Through-Thickness Center-Notched Specimens (SL)

Flaw size, 2a, mm (in.)		Stress, MN/m^2 (ksi)	Stress intensity, $MN/m^{3/2}$ (ksi $\sqrt{in.}$)		Comments
26.2	(1.03)	77.9 (11.3)	23.5	(21.4)	No SCC
18.3	(0.72)	95.8 (13.9)	24.0	(21.9)	No SCC
27.9	(1.10)	89.6 (13.0)	27.9	(25.4)	SCC, 2.5 mm (0.1 in.)

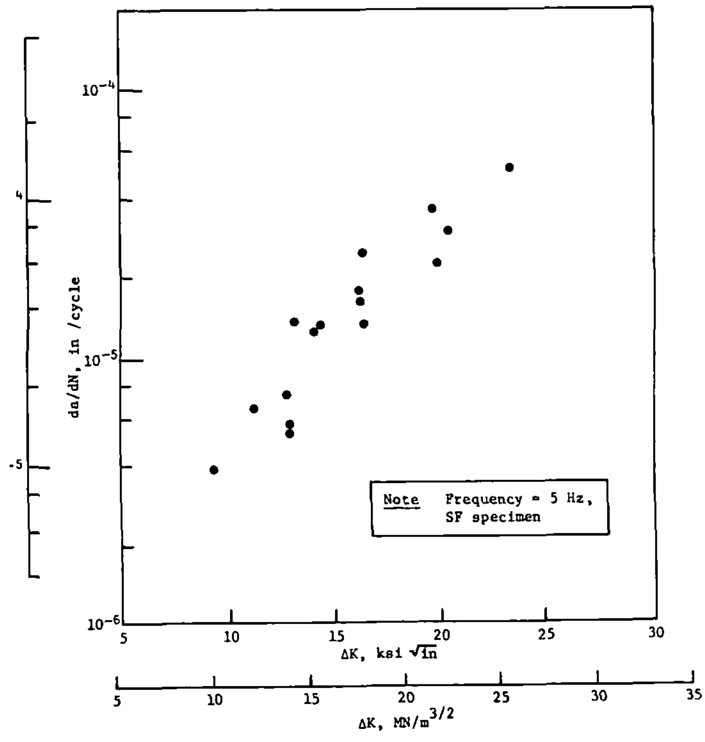

Figure 22.- Cyclic crack growth for longitudinal 2124-T851 in air (SF)

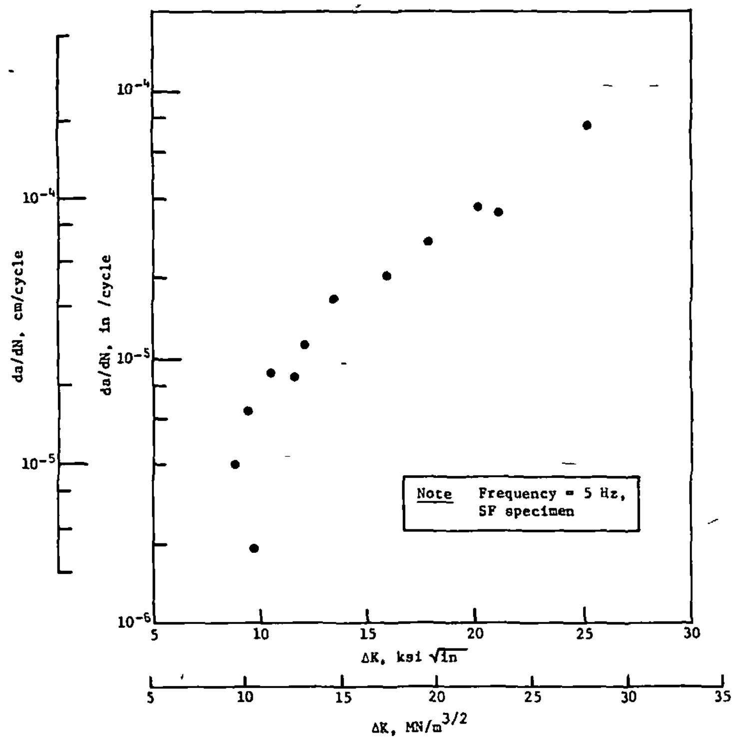

Figure 23.- Cyclic crack growth for longitudinal 2124-T851 in 3.5% NaCℓ (SF)

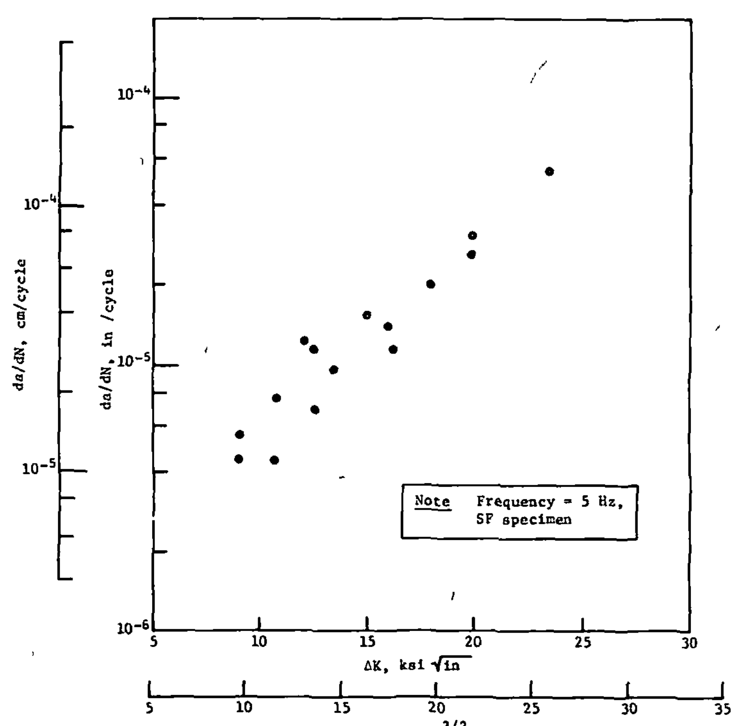

Figure 24.- Cyclic crack growth for transverse 2124-T851 in air (SF)

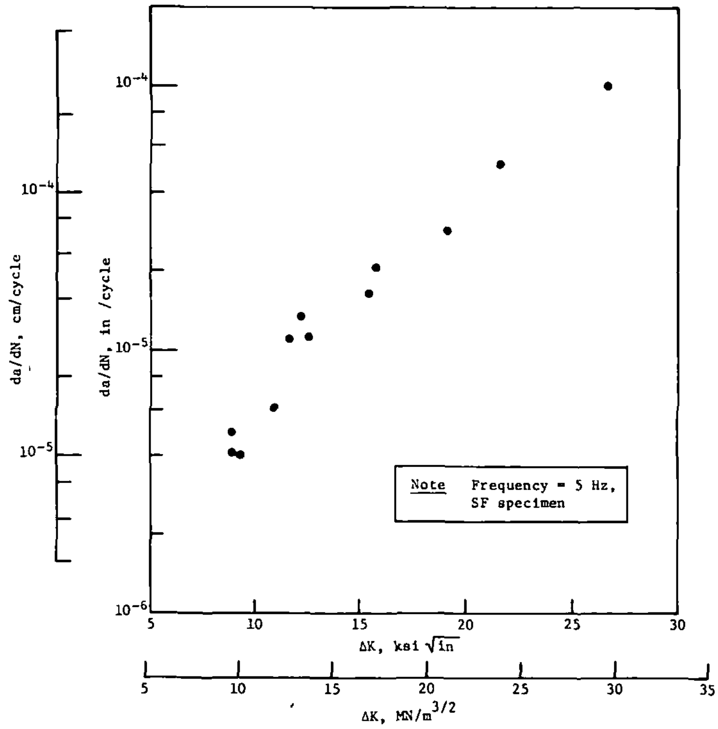

Figure 25.- Cyclic crack growth for transverse 2124-T851 in 3.5% NaCℓ (SF)

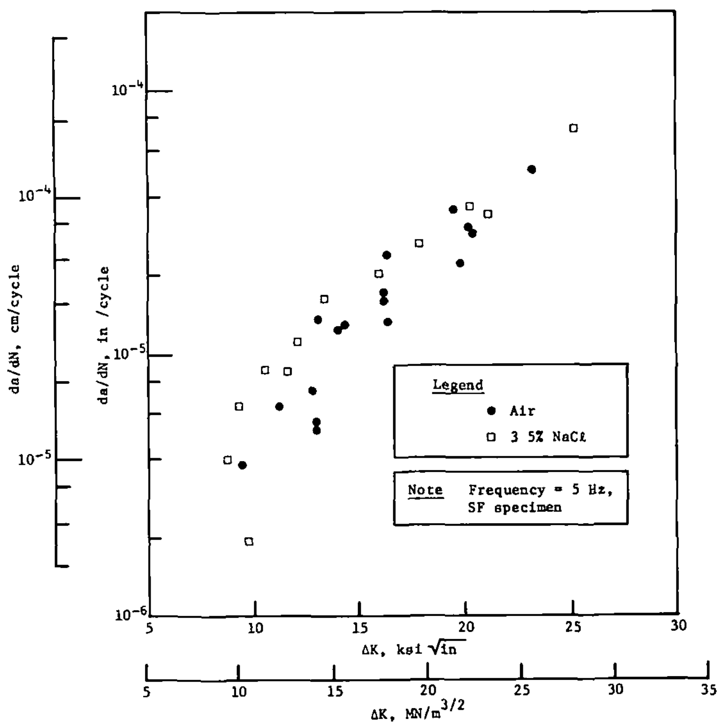

Figure 26.- Effect of environment on crack growth for longitudinal 2124-T851

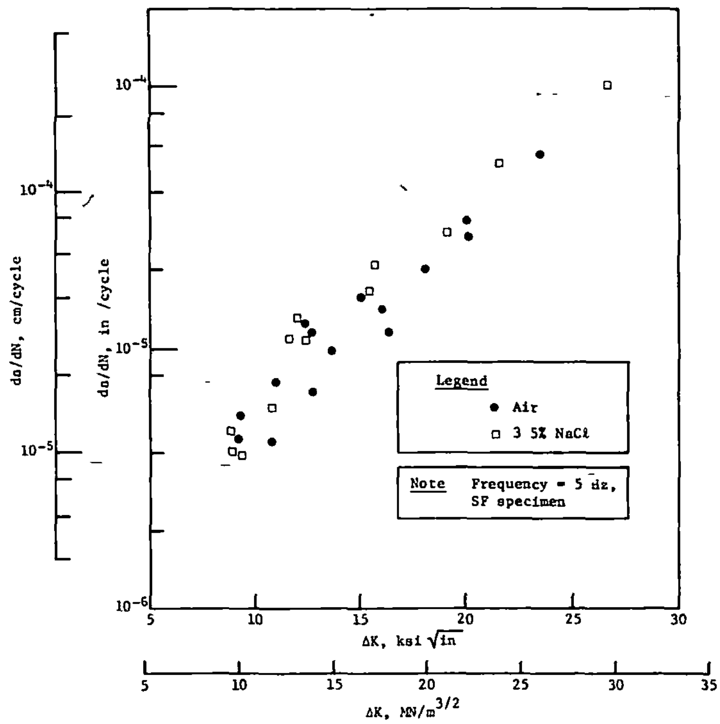

Figure 27.- Effect of environment on crack growth for transverse 2124-T851

Flaw growth data using compact specimens are presented in figures 28 through 33 for tests performed in air. Curves are based on evaluation of three specimens per condition. Testing was performed at 5 Hz except for two specimens (one each of the SL and LS orientation). These specimens were tested at 20 Hz. No effect of frequency was apparent, as shown in figures 30 and 32.

Crack growth data for compact specimens evaluated in 3.5% NaCℓ solution are given in figures 34 through 39.

The data showed that the LS and TS directions exhibited the highest crack growth resistance. The SL and ST directions exhibited the lowest resistance to crack growth. Figure 40 compares the growth data for the various orientations.

In all cases, cyclic crack growth rates in 3.5% NaCℓ were greater than those obtained by testing in air.

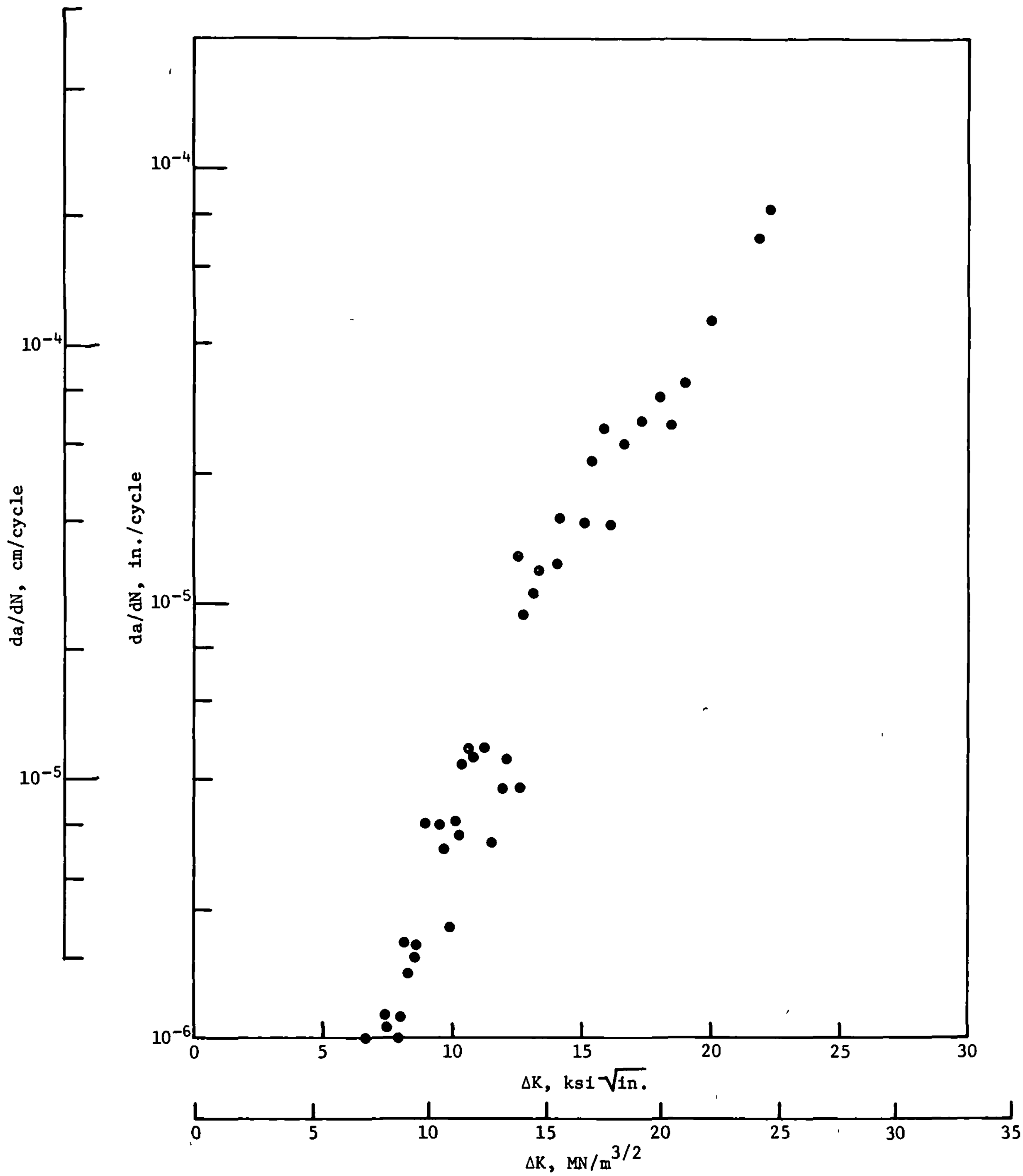

Figure 28.- Cyclic crack growth for LT specimens tested in air (CT)

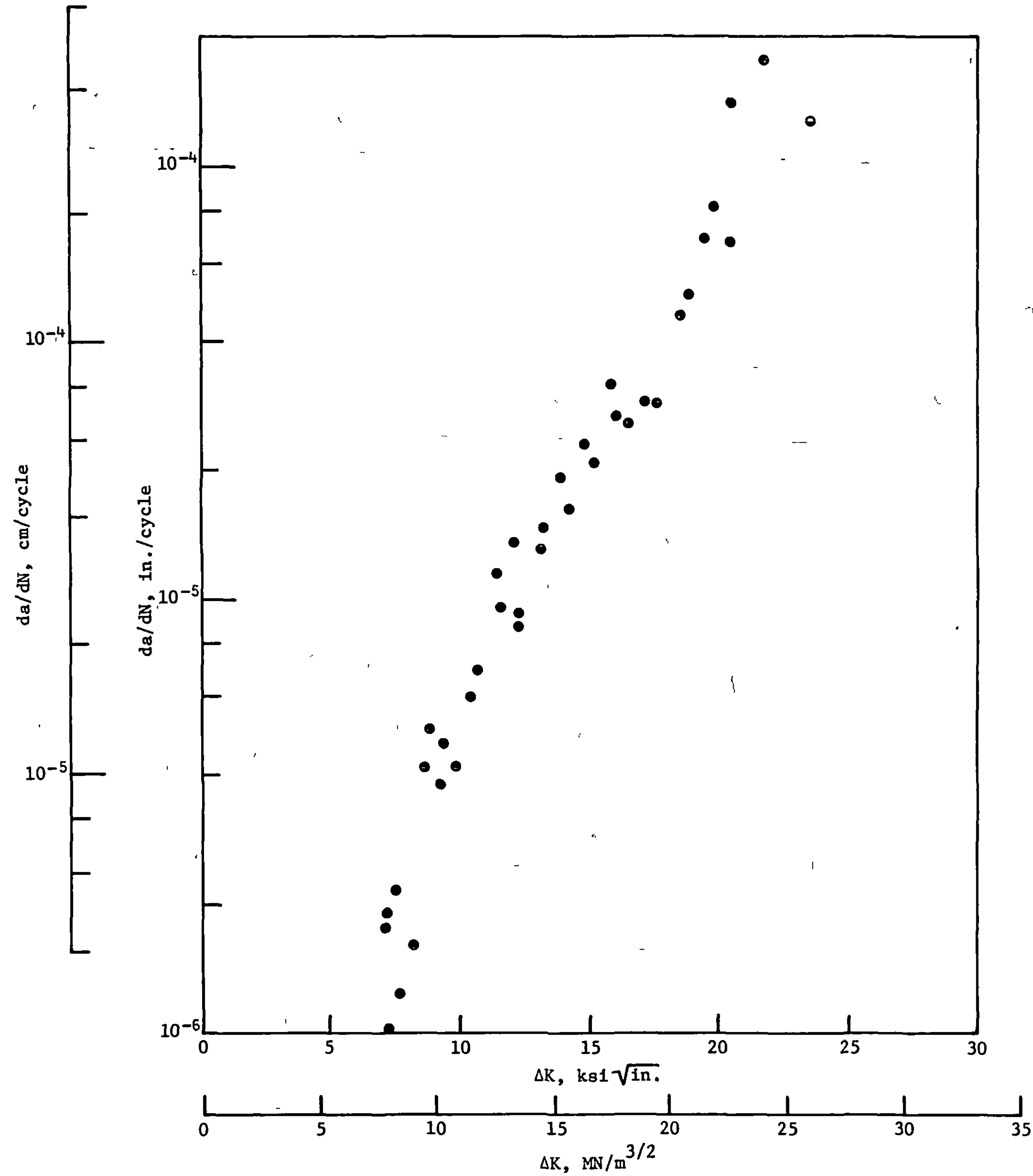

Figure 29.- Cyclic crack growth for TL specimens tested in air (CT)

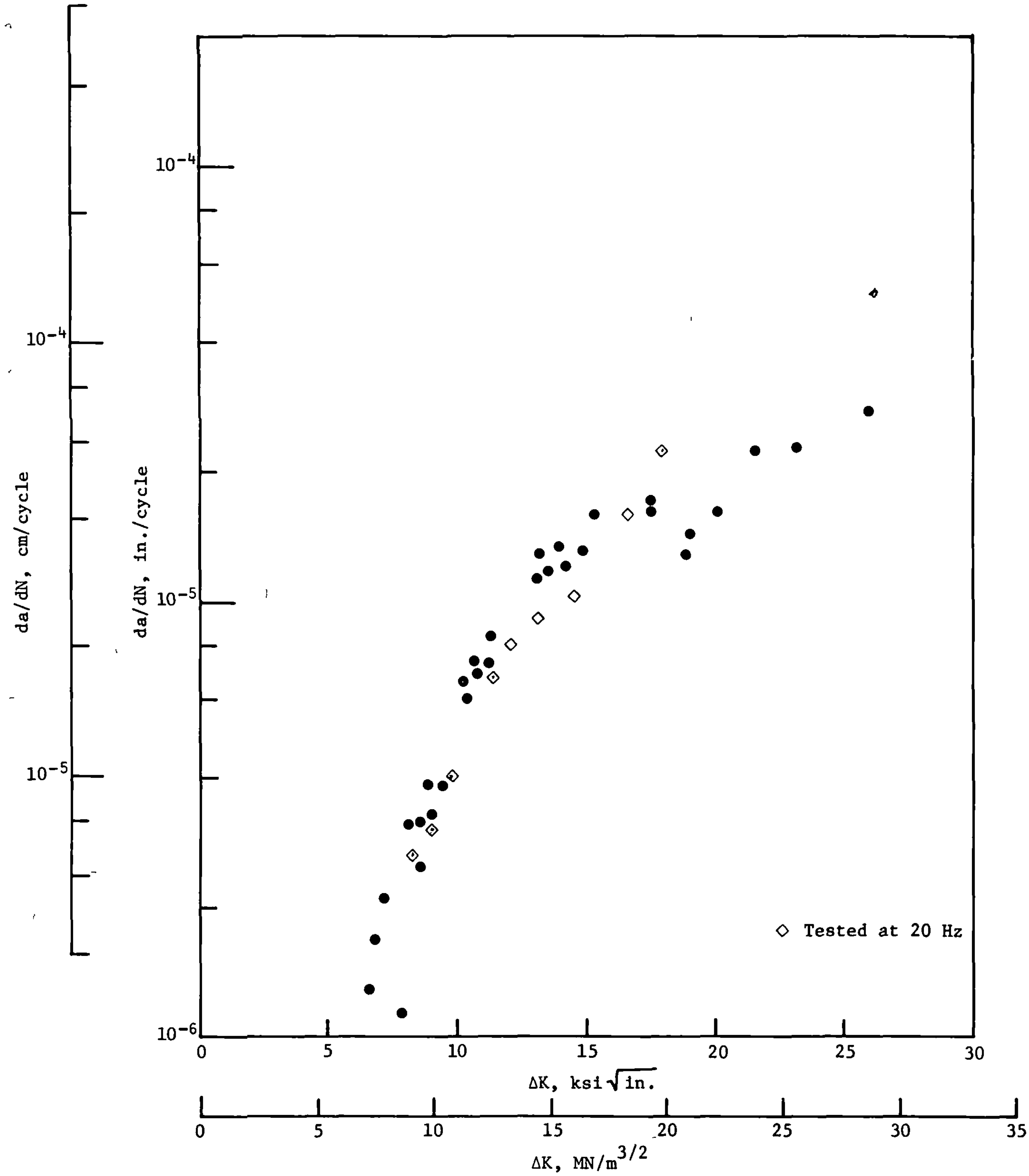

Figure 30.- Cyclic crack growth for LS specimens tested in air (CT)

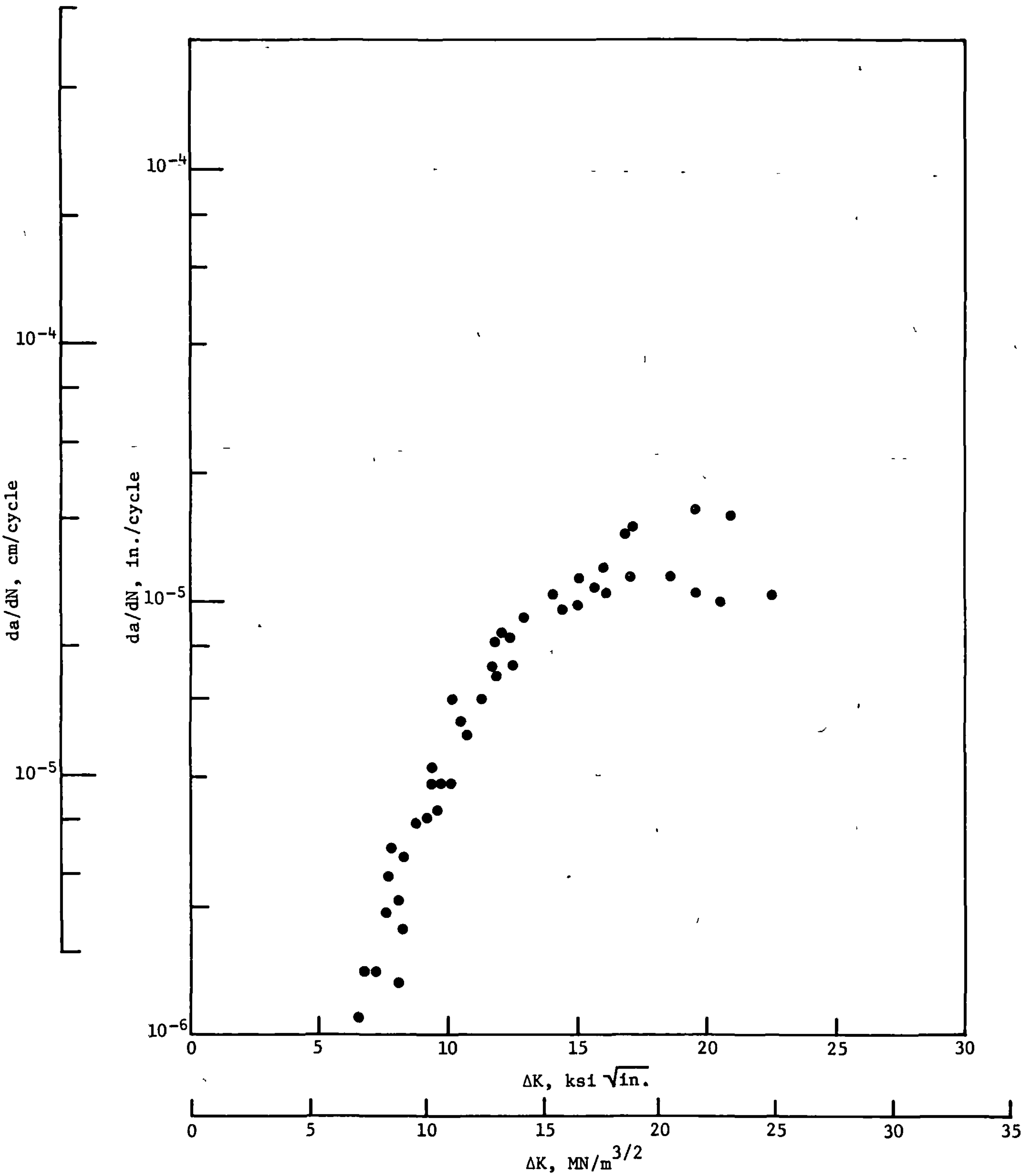

Figure 31.- Cyclic crack growth for TS specimens tested in air (CT)

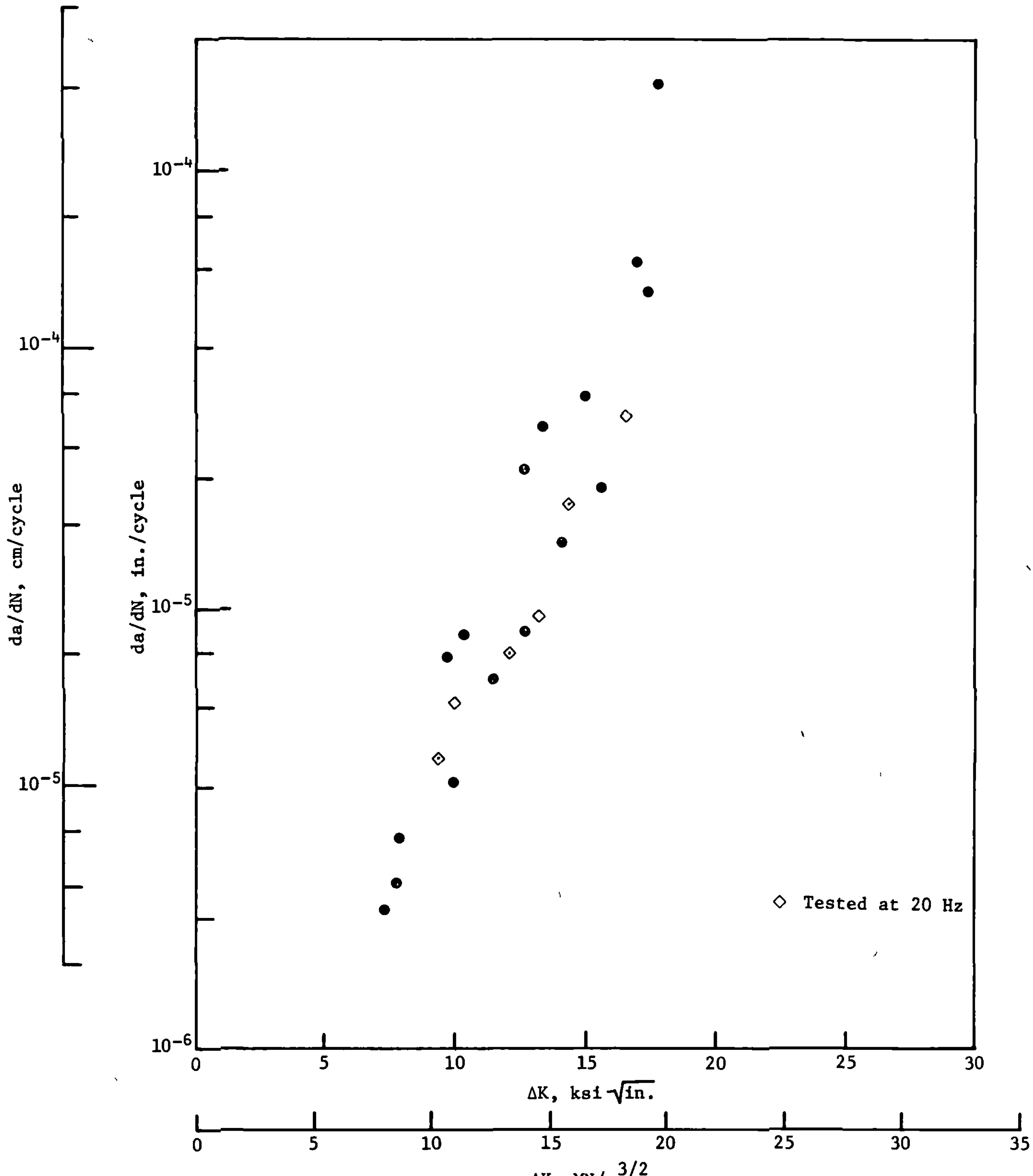

Figure 32.- Cyclic crack growth for SL specimens tested in air (CT)

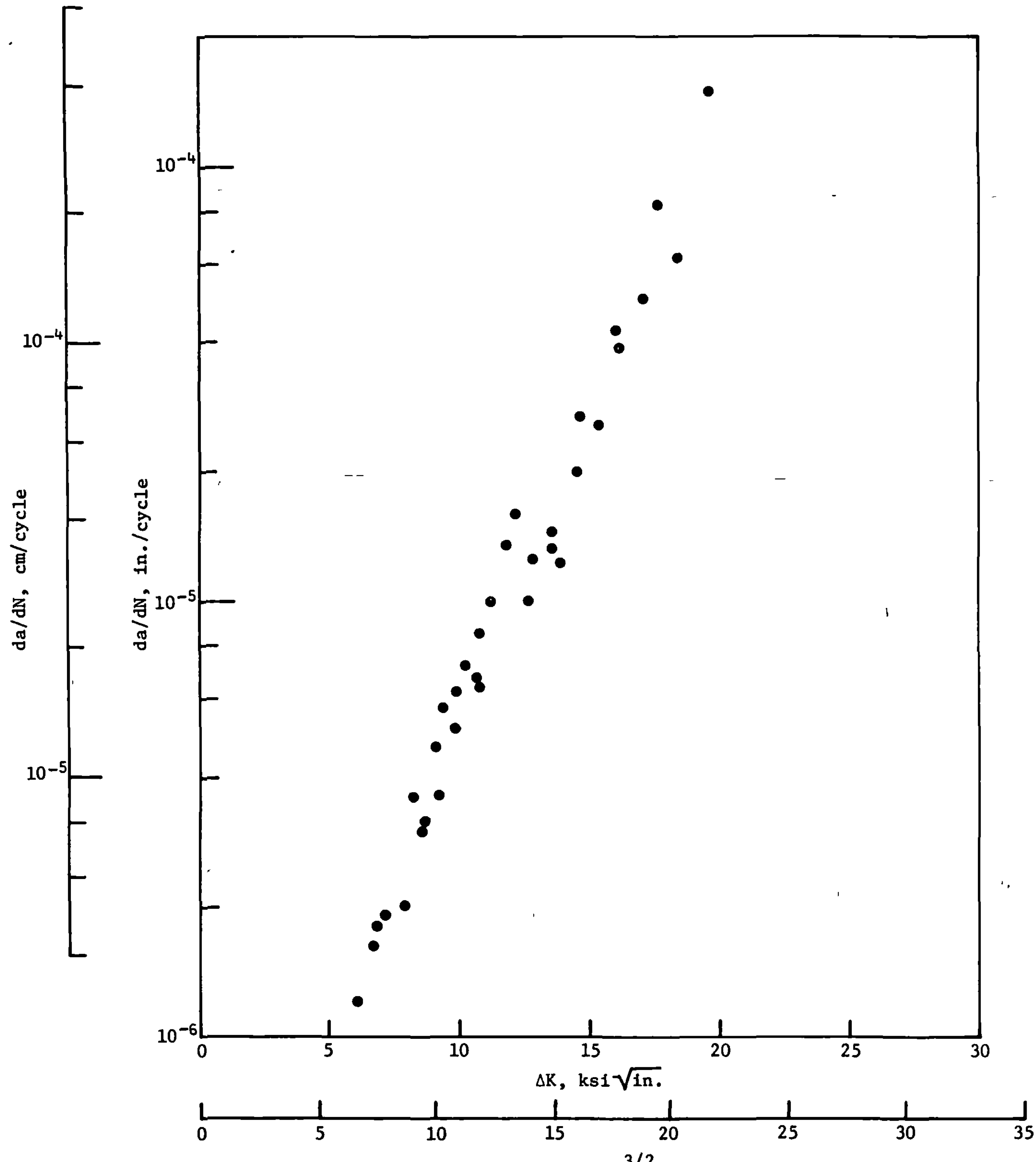

Figure 33.- Cyclic crack growth for ST specimens tested in air (CT)

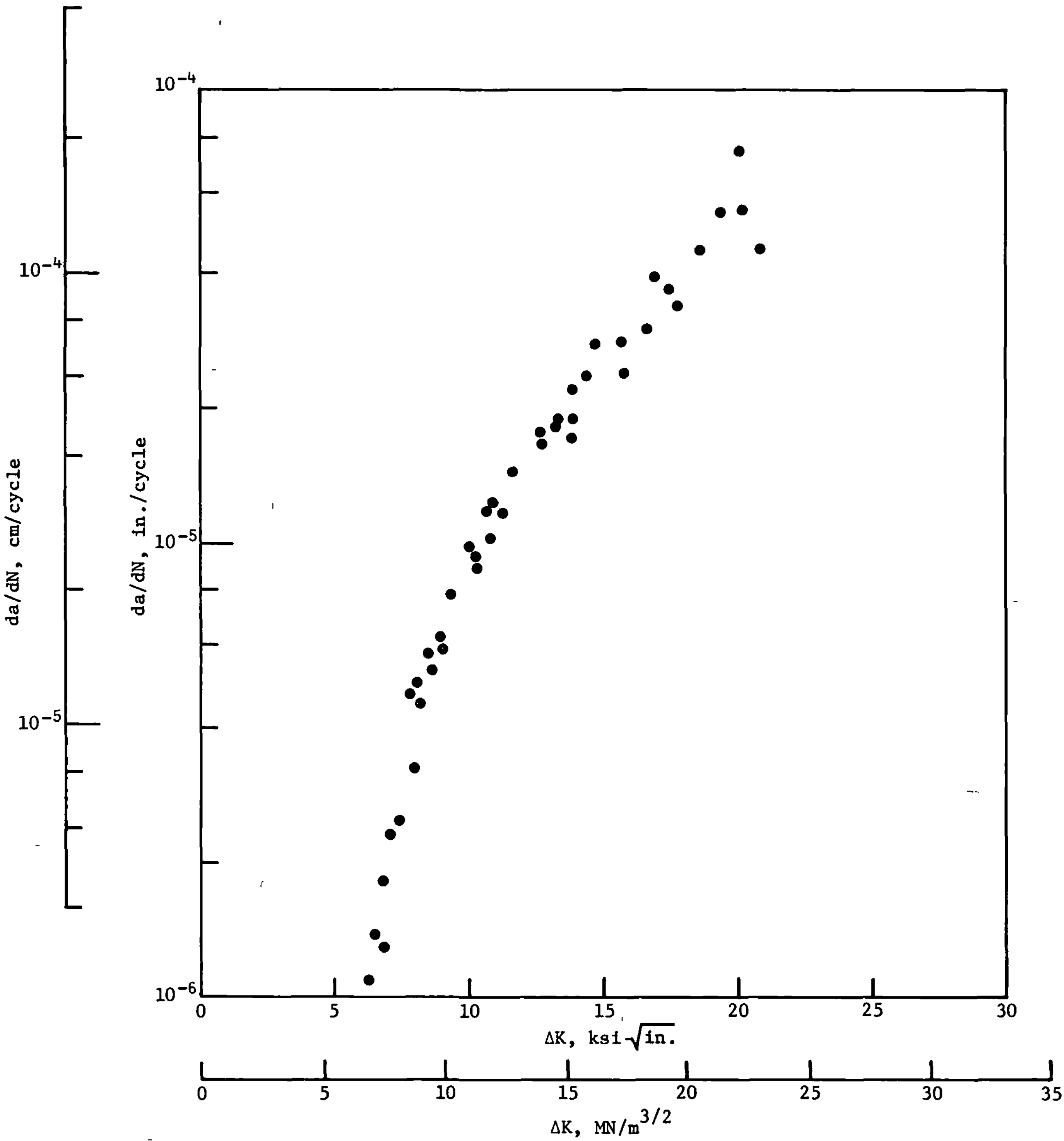

Figure 34.- Cyclic crack growth for LT specimens tested in 3.5 NaCℓ (CT)

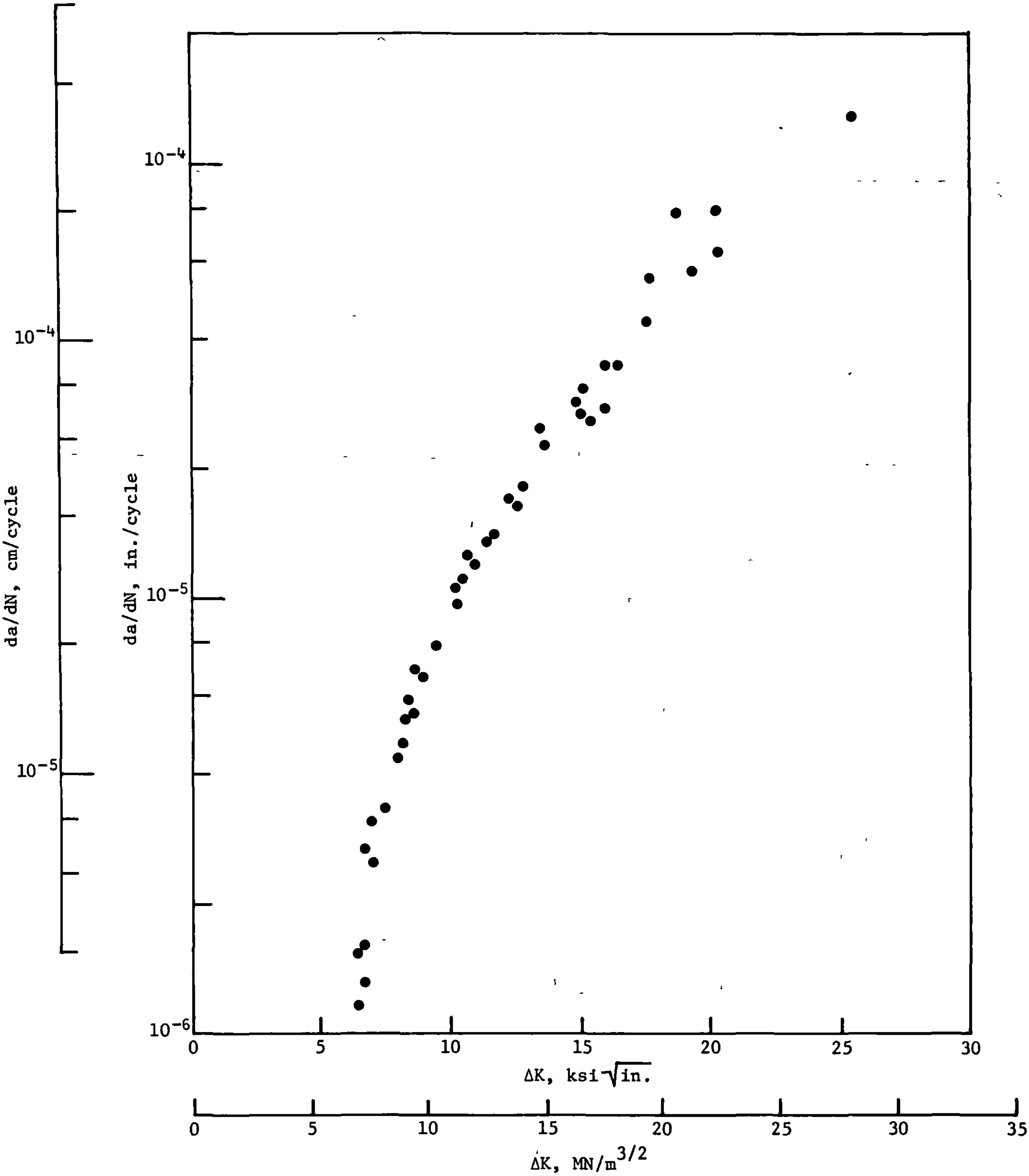

Figure 35.- Cyclic crack growth for TL specimens tested in 3.5 NaCℓ (CT)

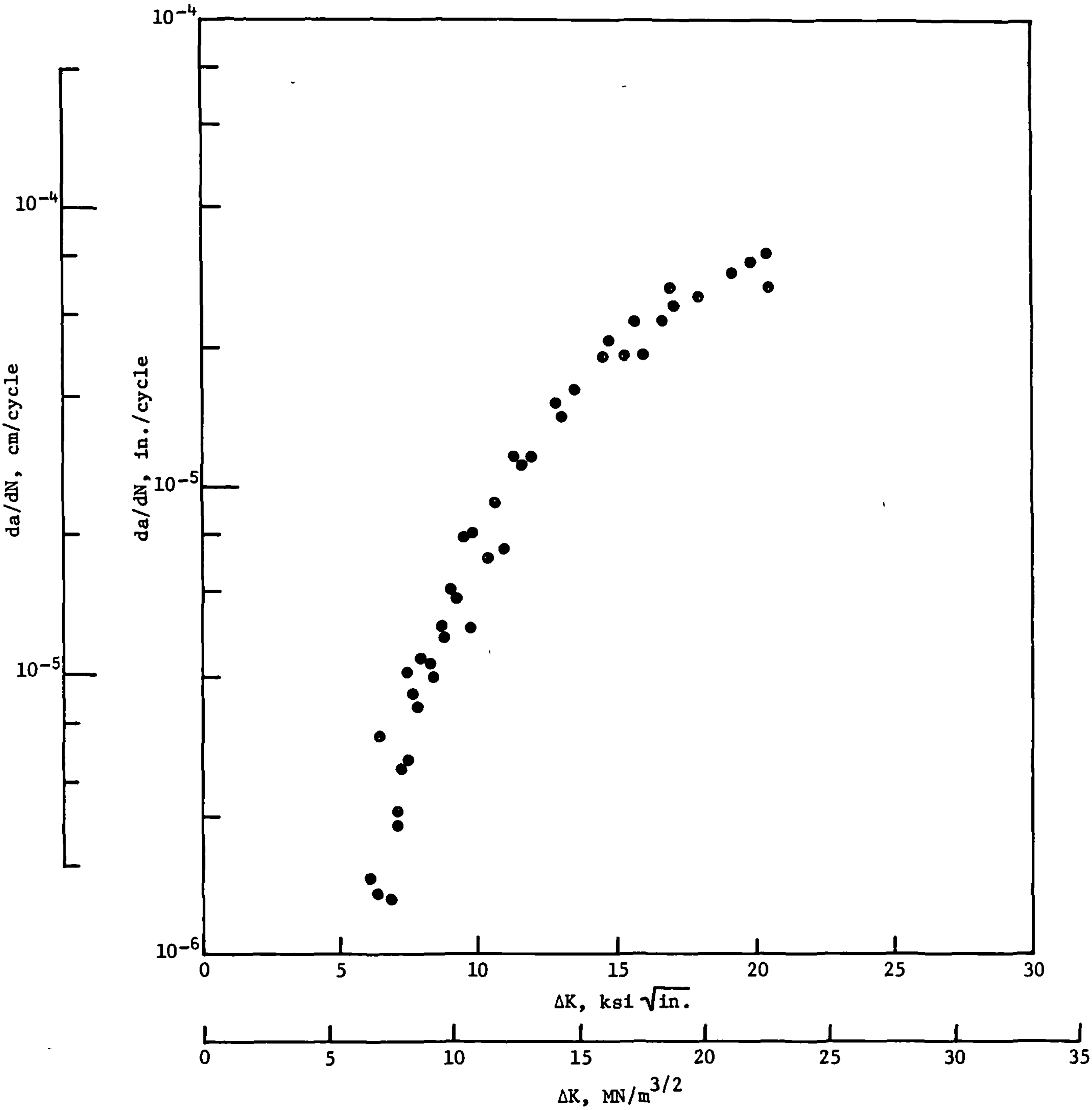

Figure 36.- Cyclic crack growth for LS specimens tested in 3.5 NaCℓ (CT)

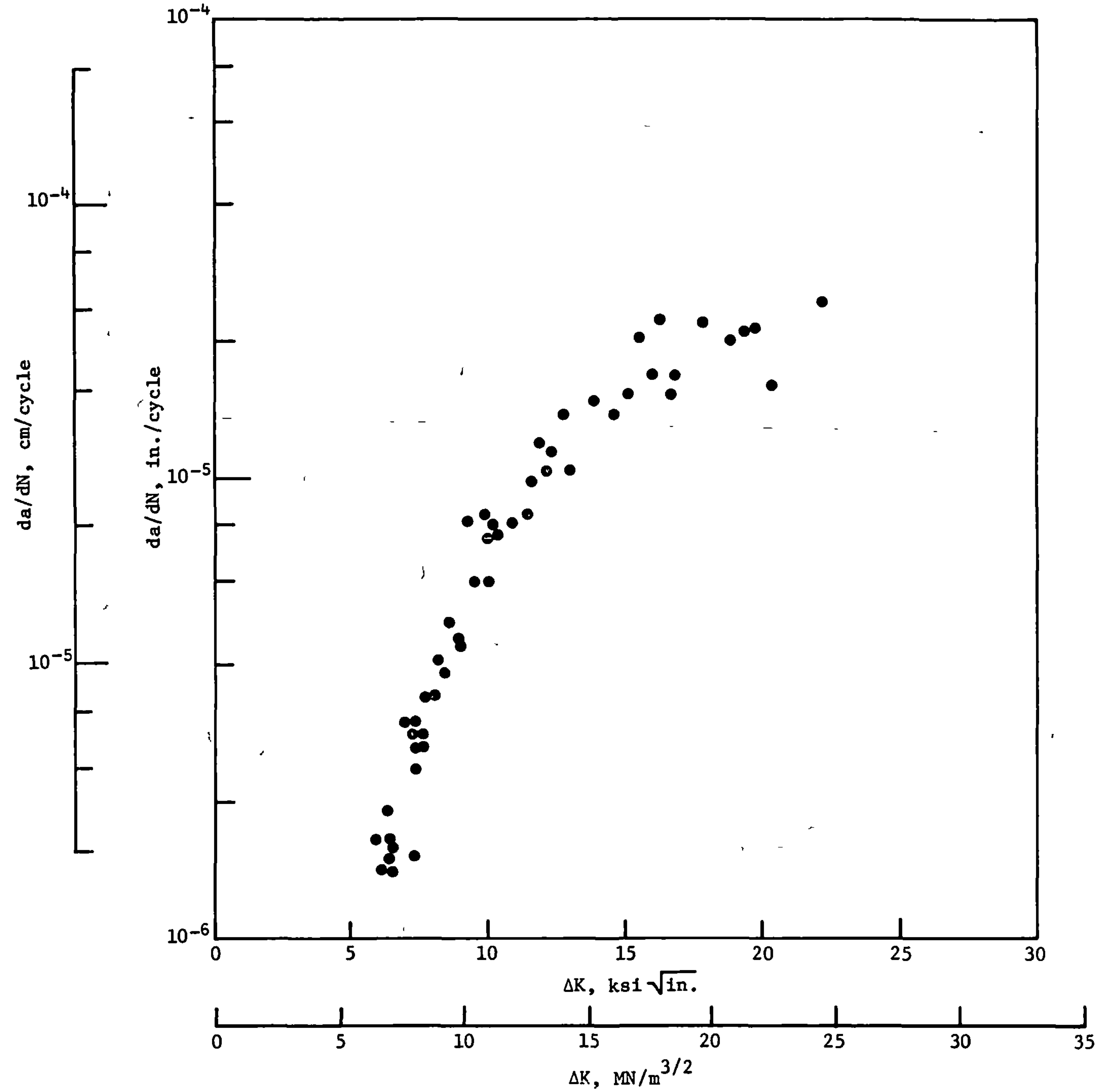

Figure 37.- Cyclic crack growth for TS specimens tested in 3.5 NaCℓ (CT)

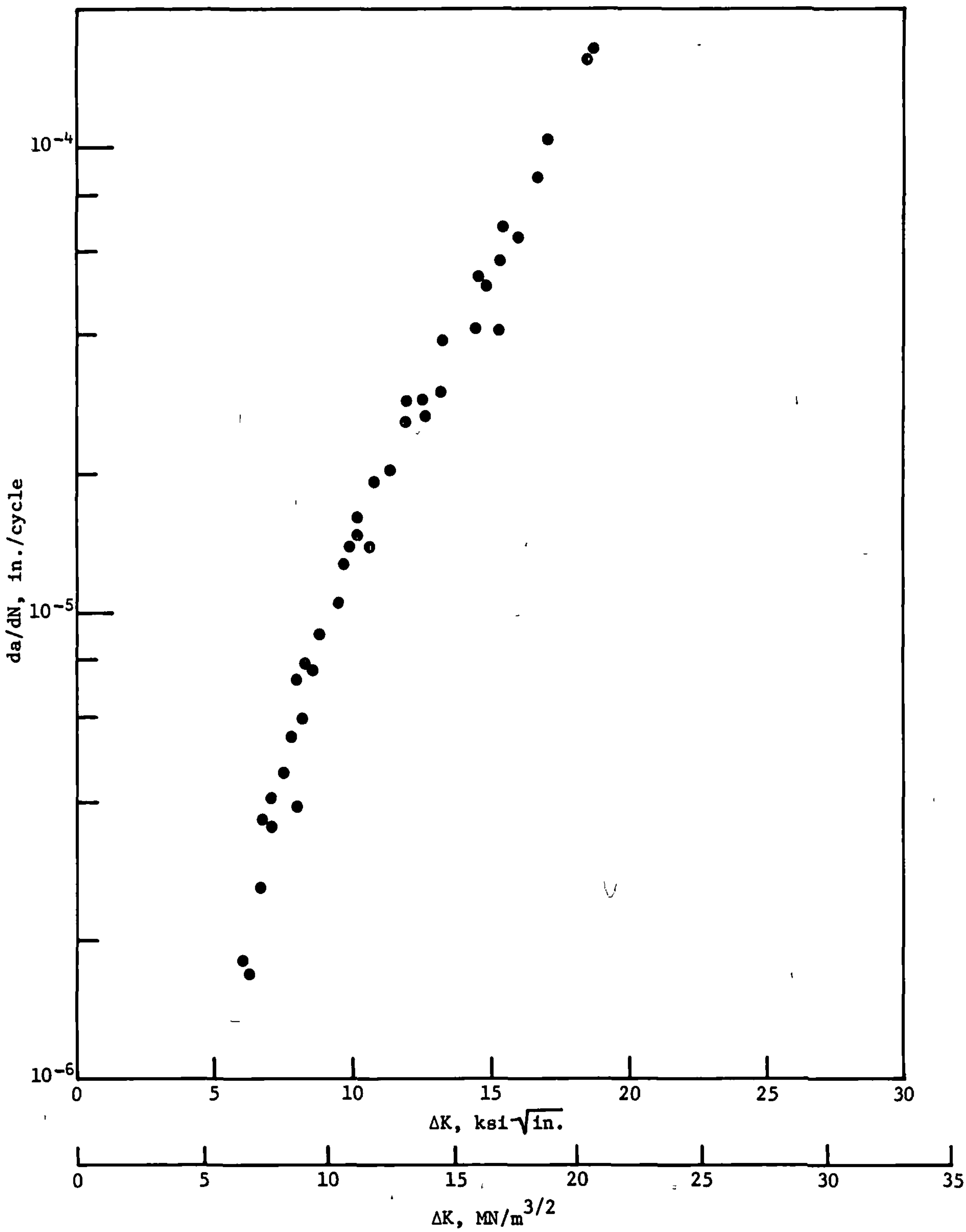

Figure 38.- Cyclic crack growth for SL specimens tested in 3.5 NaCℓ (CT)

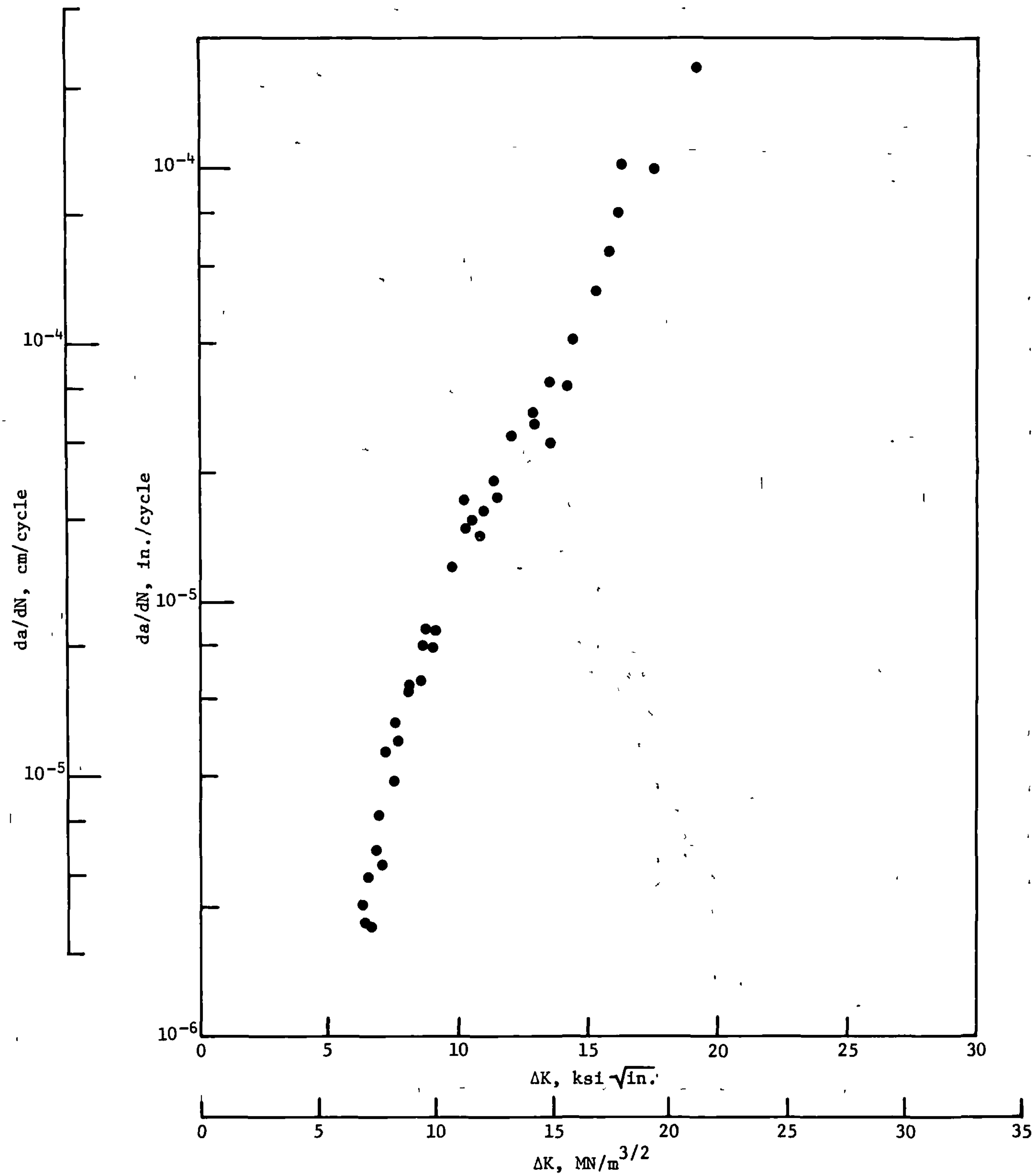

Figure 39.- Cyclic crack growth for ST specimens tested in 3.5 NaCℓ (CT)

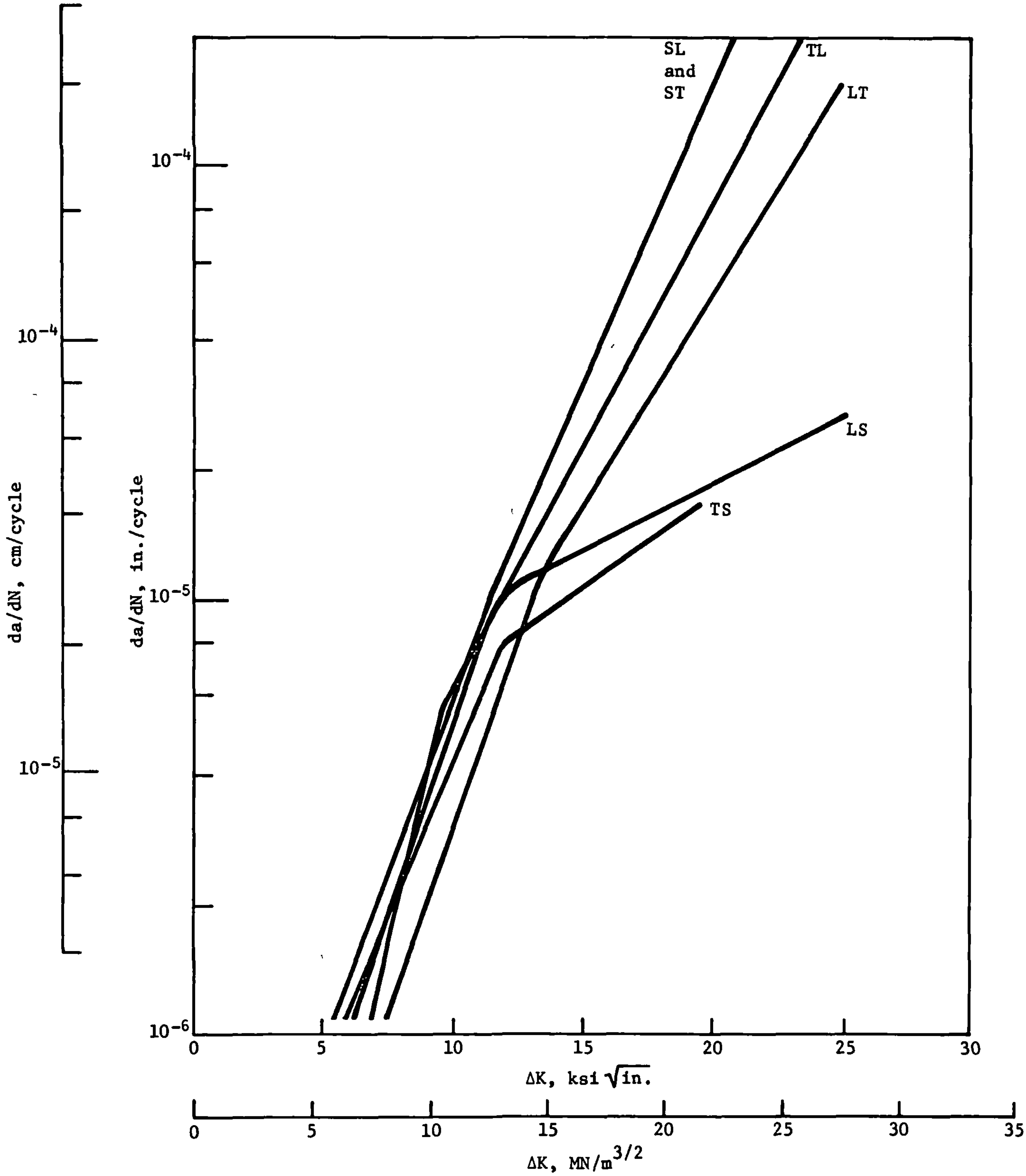

Figure 40.- Effect of specimen orientation on crack growth for CT specimens tested in air

DISCUSSION AND CONCLUSIONS

Program findings are summarized below.

- SCC was found by testing smooth specimens oriented in the short transverse direction; two types of specimens (axial and bent beam) were evaluated and provided mutual confirmation of the threshold stress level [275 MN/m^2 (40 ksi)];
- No SCC was found by evaluation of smooth specimens prepared in the longitudinal and long transverse orientations;
- Compact (CT) specimens failed to exhibit SCC after 30-day stressed exposure in any of the six orientations evaluated (LS, TS, LT, ST, SL, and TL);
- Surface-flaw (SF) specimens failed to exhibit SCC after exposure in the LS (longitudinal) and TS (long transverse) directions;
- Surface-flaw (SF) specimens and center-notch (CN) specimens prepared in the SL (short transverse) direction exhibited SCC;
- Cyclic crack growth tests showed that compact specimens oriented in the TS and LS directions exhibited greater crack growth resistance than in the other directions at stress intensity levels above 12 $MN/m^{3/2}$ (11 ksi $\sqrt{in.}$). Crack growth rates in 3.5 NaCℓ were greater than those obtained by testing in air.

The premise that SCC behavior might be stress-level-dependent as well as stress-intensity-dependent was verified. Although the tests did not quantify stress-level dependence, they established that SCC was not found at relatively high percentages of K_{Ic} in specimens with relatively low net section stress levels.

The surface flaw specimens with the welded tabs all showed SCC. However, the presence of residual stresses resulting from the electron beam welding process made interpretation of the results difficult. The two surface-flaw and three center-notched specimens evaluated with the shoulder-loading method were sufficient to bracket threshold levels.

Kaufman *et al* (ref 1) suggest that the relation between data from smooth and precracked specimens can be handled in the manner shown in figure 41. According to this concept, SCC should not occur below the horizontal line established by the smooth threshold and to the left of the stress-intensity threshold line up to the smooth stress threshold level. Another way of expressing this concept is that service stresses should not exceed the smooth stress threshold, although stress intensities might be below the threshold level.

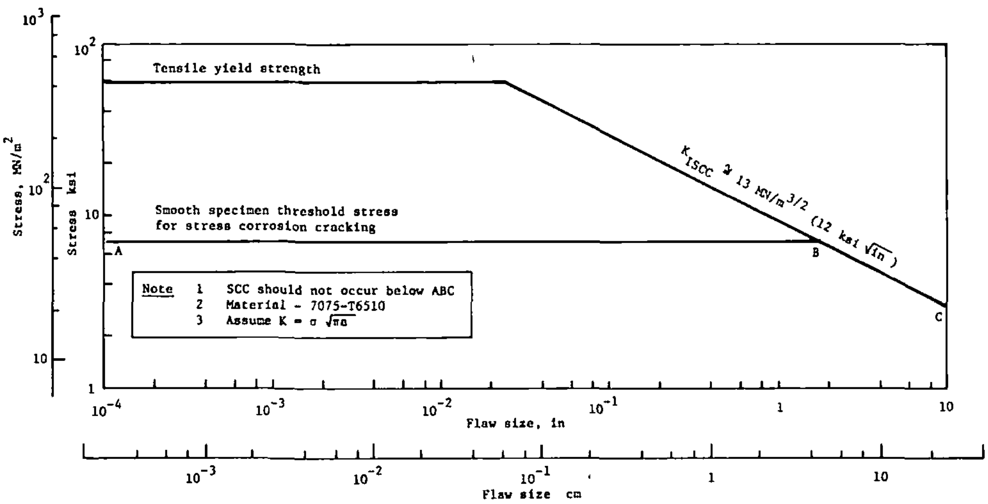

Figure 41.- Suggested method for combining stress corrosion data on smooth and precracked specimens for predicting when SCC will occur*

Data generated in this program were handled in a manner similar to that proposed by Kaufman. The scheme described below was used to plot data obtained from three types of specimen configurations. Using a logarithmic plot of stress versus flaw size, isostress intensity lines were plotted using the surface-flaw relationship. The flaw size axis is therefore a/Q rather than a. The compact data were plotted on this graph by assuming that, for the edge-type crack, the a/2C ratio approaches zero and therefore Q = 1. By plotting the crack size against the stress intensity, a stress-level value was obtained that can be considered an equivalent stress for the crack size. Surface-flaw and center-notch results for the shoulder-loaded specimens can be directly plotted as the stress-versus-crack size. Finally, the smooth data were plotted at the extreme left side of the plot corresponding to a low value of flaw size. The resulting graph is presented in figure 42.

A threshold line was drawn on the graph between the appropriate surface-flaw and center-notch specimen points. The line falls at the top of the region representing the SL and ST compact specimens that did not exhibit SCC. The data indicate a defect size-dependent threshold stress-controlled behavior. However, the slope of the line is not the -1/2 that would represent the inverse square-root relationship indicative of stress-intensity-controlled behavior.

The question of why this behavior has not previosly been observed can be explained by the fact that the alloys extensively evaluated, e.g., 7075-T6, have such a low threshold stress that the SCC would occur in the compact specimen type . For alloys of intermediate corrosion resistance, the theshold stress level appears to be in the range where fracture mechanics-type testing techniques may be discriminatory.

Aluminum alloy 2124-T851 in plate gages has a moderately high resistance to stress corrosion attack. The questions regarding stress-intensity theshold will require additional investigation to develop a fuller understanding of the nature of such behavior.

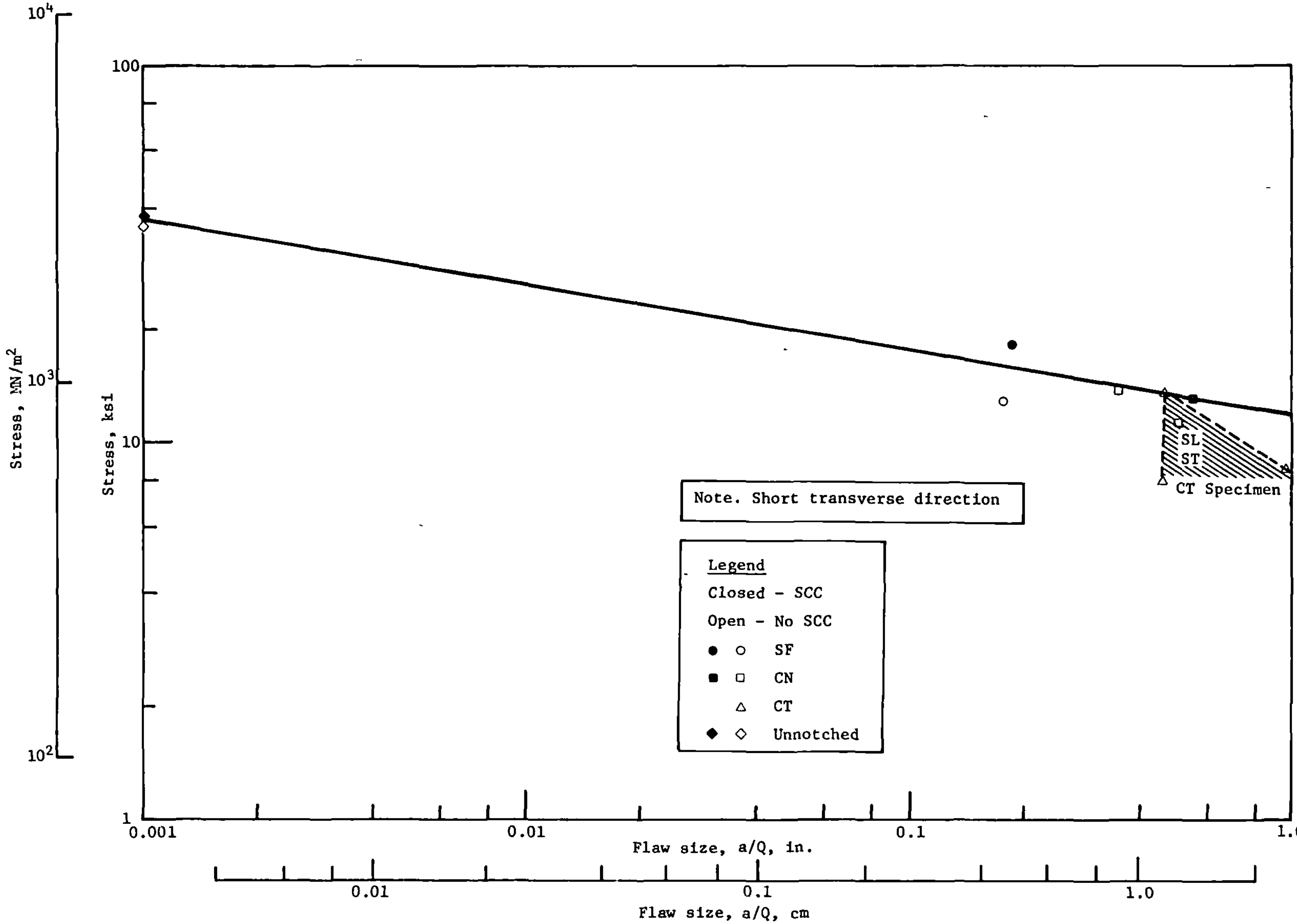

Figure 42.- Stress vs flaw size plot for 2124-T851 aluminum alloy plate

SYMBOLS

a	- Crack depth (SF specimen) or crack length (CT specimen)
2a	- Crack length (CN specimen)
a/W	- Ratio of crack length to beam width
2C	- Crack width (SF specimen)
CN	- Center-notch specimen
CT	- Compact or compact tension specimen
Hz	- Frequency in cycles per second
K_{Ic}	- Critical stress intensity factor for fracture
K_{Ii}/K_{Ic}	- Ratio of initial stress intensity to critical value
K_{ISCC}	- Stress intensity threshold for stress corrosion cracking
Q	- Flaw-shape correction factor
SCC	- Stress corrosion cracking
SF	- Surface-flaw specimen
σ_{TH}	- Stress threshold for stress corrosion cracking

REFERENCES

1. J. G. Kaufman *et al*: *Fracture Toughness, Fatigue and Corrosion Characteristics of X7080-T7E41, 7178-T651 Plate and 7075-T6510, 7075-T73S10, X7080-TE42, and 7178-T6510 Extruded Shapes.* AFML-TR-69-255, November 1969.
2. D. O. Sprowels and R. H. Brown: *Resistance of Wrought High-Strength Aluminum Alloys to Sress Corrosion.* Alcoa Technical Paper 17, 1962
3. J. Mulherin: *Stress Corrosion Testing Methods.* ASTM STP 425, 1967.

DISTRIBUTION LIST

	No. of Copies
NASA Lewis Research Center 21000 Brookpark Road Cleveland, OH 44135	
Attn: Contracting Officer, MS 500-313	1
Technical Report Control Office, MS 5-5	1
Technical Utilization Office, MS 3-16	1
AFSC Liaison Office, MS 501-3	1
Library, MS 60-3	1
R. H. Johns, MS 49-3	1
G. T. Smith, MS 49-3	34
M&S Contract File, MS 49-1	1
T. W. Orange, MS 49-3	1
National Aeronautics & Space Administration Washington, DC 20546	
Attn: KT/Technology Utilization Office	1
Library	1
RWS/D. A. Gilstad	1
NASA Scientific and Technical Information Facility P.O. Box 8757 Baltimore/Washington International Airport, MD 21240	
Attn: Accessioning Department	10
NASA-Ames Research Center Moffett Field, CA 94035	
Attn: Library	1
D. Williams	1
NASA-Flight Research Center P.O. Box 278 Edwards, CA 93523	
Attn: Library	1
NASA-Goddard Space Flight Center Greenbelt, MD 20771	
Attn: Library	1
NASA-John F. Kennedy Space Center Kennedy Space Center, FL 32931	
Attn: Library	1

NASA-Langley Research Center
Hampton, VA 23365

Attn: Library	1
R. W. Leonard	1
H. Hardrath	1
W. Elber	1

NASA-Manned Spacecraft Center
Houston, TX 77001

Attn: Library	1
R. E. Johnson	1
S. V. Glorioso	1
R. Forman	1

NASA-Marshall Space Flight Center
Marshall Space Flight Center, AL 35812

Attn: Library	1
S&E-ASTN/AA/C. Lifer	1
S&E-ASTN/ASR/C. Crockett	1
S&E-ASTN/AS/H. Coldwater	1

Air Force Office of Scientific Research
Washington, DC 20333

Attn: Library	1

Air Force Rocket Propulsion Laboratory (RPM)
Edwards, CA 93523

Attn: Library	1

Air Force Systems Command
Aeronautical Systems Division
Wright-Patterson AFB, OH 45433

Attn: Library	1
C. F. Tiffany, Code ENF	1

Air Force Systems Command
Andrews Air Force Base
Washington, DC 20332

Attn: Library	1

Wright-Patterson Air Force Base
Wright-Patterson Air Force Base, OH 45433

Attn: AFML Library	1
D. M. Forney	1

Wright-Patterson Air Force Base
Wright-Patterson Air Force Base, OH 45433

Attn: AFFDL/H. A. Wood	1

Department of the Army
U.S. Army Material Command
Washington, DC 20315
Attn: AMCPD-RC 1

Commanding Officer
U.S. Army Research Office (Durham)
Box CM, Duke Station
Durham, NC 27706
Attn: Library 1

Bureau of Naval Weapons
Department of the Navy
Washington, DC 20360
Attn: RRRE-6 1

Brown University
Providence, RI 02912
Attn: Technical Library 1
J. R. Rice (Dr.) 1

Case Western Reserve University
10090 Euclid Avenue
Cleveland, OH 44115
Attn: Technical Library 1

Carnegie Institute of Technology
Department of Civil Engineering
Pittsburgh, PA 15213
Attn: Library 1

Colorado State University
Department of Mechanical Engineering
Ft. Collins, CO 80521
Attn: F. Smith (Dr.) 1

Cornell University
Department of Materials Science and Engineering
Ithaca, NY 14830
Attn: Library 1

Pennsylvania State University
State College, PA 16802
Attn: Library 1

Purdue University
W. Lafayette, IN 47906
Attn: Library 1
C. T. Sun 1

University of Denver
Denver Research Institute
P.O. Box 10126
Denver, CO 80210
Attn: Security Office 1

Aerospace Corporation
2400 E. El Segundo Boulevard
Los Angeles, CA 90045
Attn: Library-Documents 1

Bell Aerosystems, Inc.
Box 1
Buffalo, NY 14240
Attn: J. Davis 1

Brunswick Corporation
Defense Products Division
P.O. Box 4594
43000 Industrial Avenue
Lincoln, NE 68504
Attn: Library 1

Chrysler Corporation
Space Division
P.O. Box 29200
New Orleans, LA 70129
Attn: P. Munafo 1
Library 1

Del Research Corporation
427 Main Street
Hellertown, PA 18055
Attn: P. Paris (Dr.) 1

Del West Associates, Inc.
6324 Variel Avenue
Suite C
Woodland Hills, CA 91364
Attn: M. Creager (Dr.) 1

General American Transportation Corporation
General American Research Division
7449 N. Natchez Avenue
Niles, IL 60648
Attn: R. N. Johnson (Dr.) 1

Commander
U.S. Naval Ordnance Laboratory
White Oak
Silver Spring, MD 20910
Attn: Library 1

Director, Code 6180 U.S. Naval Research Laboratory Washington, DC 20390 Attn: Library	2
H. W. Carhart	1
J. M. Krafft	1
Atomic Energy Commission Division of Reactor Development and Technology Washington, DC 20767	1
National Science Foundation Engineering Division 1800 G Street, NW Washington, DC 20540 Attn: Library	1
Denver Federal Center U.S. Bureau of Reclamation - Translation Group P.O. Box 25007 Denver, CO 80225 Attn: P. M. Lorenz	2
Battelle Memorial Institute 505 King Avenue Columbus, OH 43201 Attn: Library	1
E. Hulbert (Dr.)	1
G. Hahn (Dr.)	1
C. Bell (Dr.)	1
IIT Research Institute Technology Center Chicago, IL 60616 Attn: Library	1
Stanford Research Institute 3333 Ravenswood Avenue Menlo Park, CA 94025 Attn: Library	1
Martin Marietta Corporation P.O. Box 29304 New Orleans, LA 70189 Attn: Donald Bolsted	1
McDonnell Douglas Aircraft Corporation P.O. Box 516 Lambert Field, MO 63166 Attn: Library	1
L. J. Pionke	1
B. V. Whiteson	1

McDonnell Douglas Astronautics	
Western Division	
5301 Bolsa Avenue	
Huntington Beach, CA 92647	
Attn: Library	1
H. Babel	1
R. Rawe	1
North American Rockwell Space Division	
12214 Lakewood Boulevard	
Downey, CA 90241	
Attn: J. E. Colipriest	1
Northrop Space Laboratories	
3901 West Broadway	
Hawthorne, CA 90250	
Attn: Library	1
A. F. Liu (Dept. 3853, Zone 82)	1
North American Rockwell, Inc.	
Rocketdyne Division	
6633 Canoga Avenue	
Canoga Park, CA 91304	
Attn: Library, Dept. 596-306	1
G. Vorman	1
General Dynamics	
P.O. Box 748	
Ft. Worth, TX 76101	
Attn: Library	1
C. D. Little	1
General Dynamics/Convair Aerospace	
P.O. Box 1128	
San Diego, CA 92112	
Attn: Library	1
J. Jensen	1
W. Witzel	1
J. Haskins	1
Grumman Aircraft Engineering Corporation	
Bethpage, Long Island, NY 11714	
Attn: Library	1
Jet Propulsion Laboratory	
4800 Oak Grove Drive	
Pasadena, CA 91103	
Attn: Library	1
J. Lewis	1

Ling-Temco-Vought Corporation
P.O. Box 5907
Dallas, TX 75222
Attn: Library 1
R. Goolsby 1
S. Ranganath 1

Lockheed Missiles and Space Company
P.O. Box 504
Sunnyvale, CA 94087
Attn: Library 1
R. E. Lewis 1

Republic Aviation
Fairchild Hiller Corporation
Farmingdale, Long Island, NY 11735
Attn: Library 1

Thiokol Chemical Corporation
Wasatch Division
P.O. Box 524
Brigham City, UT 84302
Attn: Library Section 1

TRW Systems, Inc.
One Space Park
Redondo Beach, CA 90278
Attn: Technical Library, Document Acquisitions 1

United Aircraft Corporation
Corporate Library
400 Main Street
East Hartford, CT 06108
Attn: Library 1

United Aircraft Corporation
Pratt and Whitney Division
Florida Research and Development Center
P.O. Box 2691
West Palm Beach, FL 33402
Attn: Library 1

Westinghouse Research Laboratories
Beulah Road, Churchill Borough
Pittsburgh, PA 15235
Attn: Library 1
W. K. Wilson 1
G. T. Wessel 1

Massachusetts Institute of Technology
Cambridge, MA 02138
Attn: Library 1